Integration of Concentrated Solar Power Plants in Renewable-Only VPP with Electrical and Thermal Demands: A Two-Stage Robust Bidding Approach

Hadi Nemati*, Pedro Sánchez-Martín, Álvaro Ortega, Lukas Sigrist, Luis Rouco

Comillas Pontifical University ICAI School of Engineering, Institute for Research in Technology, Madrid, Spain

*Corresponding author

E-mail address: hnemati@comillas.edu

Abstract

This paper proposes the integration of Concentrated Solar Power Plant (CSP) in the Renewable-only virtual power plant (RVPP) for bidding in the electricity day-ahead and secondary reserve markets, as well as trading thermal energy through a heat purchase agreement. A reformulated two-stage robust optimization approach is introduced to account for multiple uncertainties, including electricity prices, non-dispatchable renewable energy sources' electrical production, CSP thermal production, and uncertainties in electrical and thermal demand consumption. The provision of energy and reserve by the thermal storage of CSP is modeled using an adjustable approach, which allocates a share of energy for up and down reserves based on the profitability of the RVPP. Simulations are conducted for several case studies to demonstrate the effectiveness and computational efficiency of the proposed approach under different RVPP operator decisions against uncertain parameters and various trading strategies for electricity and thermal energy. The simulation results show that integrating CSP into RVPP enhances RVPP flexibility for both electrical and thermal trading. Furthermore, the results indicate that the profitability of the RVPP increases when all trading options are considered, across different levels of conservatism adopted by the RVPP operator in response to uncertain parameters.

Keywords

Concentrated solar power plant, virtual power plant, thermal storage, electricity markets, heat purchase agreement, robust optimization

Abbreviations

Acronym	Definition	Acronym	Definition
aFRR	Automatic Frequency Restoration Reserve	PDF	Probability Density Function
ARO	Adaptive Robust Optimization	PTC	Parabolic Trough Collectors
ASM	Ancillary Service Market	PV	Photovoltaic
BAM	Balancing Market	PVT	Photovoltaic-Thermal
CAES	Compressed Air Energy Storage	RES	Renewable Energy Source
C&CG	Column & Constraint Generation	RO	Robust Optimization
CSP	Concentrated Solar Power Plant	RTM	Real-Time Market
CVaR	Conditional Value-at-Risk	RVPP	Renewable-only Virtual Power Plant
DAM	Day-Ahead Market	SF	Solar Field
DRO	Distributed Robust Optimization	SOS-2	Special Ordered Set of Type 2
ED	Electric Demand	SP	Stochastic Programming
EH	Electric Heater	SRM	Secondary Reserve Market
ES	Electrical Storage	TD	Thermal Demand
EV	Electric Vehicle	TS	Thermal Storage
HPA	Heat Purchase Agreement	TSO	Transmission System Operator
IDM	Intra-Day Market	VaB	Value-at-Best
IGDT	Information Gap Decision Theory	VPP	Virtual Power Plant
MILP	Mixed Integer Linear Programming	WF	Wind Farm
MO	Market Operator	ND-RES	Non-Dispatchable Renewable Energy Sources
PB	Power Block		

Nomenclature

Indexes and Sets

$d \in \mathcal{D}$	Set of EDs/TDs
$n \in \mathcal{N}$	Set of segments of piecewise efficiency function of PB of CSPs
$r \in \mathcal{R}$	Set of ND-RESs
$t \in \mathcal{T}$	Set of time periods
$t \in \mathcal{T}^{DA}$	Set of time periods in which the worst case of DAM price uncertainty occurs
$t \in \mathcal{T}^{SR,\uparrow(\downarrow)}$	Set of time periods in which the worst case of up (down) SRM price uncertainty occurs
$t \in \mathcal{T}_\theta$	Set of time periods in which the worst case of SF of CSP θ thermal production uncertainty occurs
$t \in \mathcal{T}_d$	Set of time periods in which the worst case of ED/TD d consumption uncertainty occurs
$t \in \mathcal{T}_r$	Set of time periods in which the worst case of ND-RES r electrical production uncertainty occurs
$u \in \mathcal{U}$	Set of RVPP units
$\theta \in \Theta$	Set of CSPs
Ξ^O/Ξ^C	Set of decision variables of uncertainties in the objective function/constraints of the optimization problem
$\Xi^{DA+SR+HPA}$	Set of decision variables of DAM, SRM, and HPA

Parameters

$C_{r(\theta)}$	Operation and maintenance costs of ND-RES r (CSP θ)	[€/MWh]
$\bar{E}_\theta^{TS}/\underline{E}_\theta^{TS}$	Upper/lower bound of thermal energy of TS of CSP θ	[MWh]
$\underline{E}_d/\underline{Q}_d$	Minimum electrical/thermal energy consumption of ED/TD d throughout the operation horizon	[MWh]
$\bar{H}_d/\underline{H}_d$	Upper/lower bound of thermal power consumption of TD d	[MW]
$\check{H}_{d,t}/\hat{H}_{d,t}$	Lower bound/positive deviation of the TD d consumption forecast during period t	[MW]

K_θ^{PB}	Start up electrical output multiplier of PB of CSP	[p.u.]
M	Big positive value	[€] or [MW]
$N_\theta^{OFF}/N_\theta^{ON}$	Number of initial periods during which turbine of CSP θ must be offline/online	[-]
$\bar{P}_d/\underline{P}_d$	Upper/lower bound of electrical power consumption of ED d	[MW]
$\bar{P}_\theta^{PB}/\underline{P}_\theta^{PB}$	Upper/lower bound of thermal power of PB of CSP θ	[MW]
$\bar{P}_\theta^{TS,+}/\underline{P}_\theta^{TS,+}$	Upper/lower bound of thermal charging power of TS of CSP θ	[MW]
$\bar{P}_\theta^{TS,-}/\underline{P}_\theta^{TS,-}$	Upper/lower bound of thermal discharging power of TS of CSP θ	[MW]
$\bar{P}_{r(\theta)}/\underline{P}_{r(\theta)}$	Upper/lower bound of electrical power production of ND-RES r (CSP θ)	[MW]
$\hat{P}_{\theta,t}^{SF}/\check{P}_{\theta,t}^{SF}$	Upper bound/negative deviation of the thermal power production forecast of SF of CSP θ during period t	[MW]
$\hat{P}_{r,t}/\check{P}_{r,t}$	Upper bound/negative deviation of the ND-RES r production forecast during period t	[MW]
$\check{P}_{d,t}/\hat{P}_{d,t}$	Lower bound/positive deviation of the ED d consumption forecast during period t	[MW]
P_u	Electrical power capacity of RVPP unit u	[MW]
$P_{\theta,n}^{PB}$	Thermal power of PB of CSP θ in segment n of piecewise function	[MW]
$P_{\theta,t}^{SF}$	Thermal power production forecast of SF of CSP θ during period t	[MW]
$P_{d,t}/H_{d,t}$	ED/TD d consumption forecast during period t	[MW]
$P_{r,t}$	ND-RES r production forecast during period t	[MW]
$\bar{R}_{r(\theta)}^{SR}/\underline{R}_{r(\theta)}^{SR}$	Up (down) secondary reserve ramp rate of ND-RES r (CSP θ)	[MW/min]
$\underline{R}_d^{SR}/\bar{R}_d^{SR}$	Up/down secondary reserve ramp rate of ED d	[MW/min]
T^{SR}	Required time for secondary reserve action	[min]
UT_θ/DT_θ	Minimum up/down time of turbine of CSP θ	[-]
$\underline{\beta}_{d,t}/\bar{\beta}_{d,t}$	Percentage of up/down flexibility of ED d during period t	[%]
Γ^{DA}	Uncertainty budget of DAM electricity price	[-]
$\Gamma^{SR,\uparrow(\downarrow)}$	Uncertainty budget of up (down) SRM electricity price	[-]
Γ_d	Uncertainty budget of consumption of ED/TD d	[-]
$\Gamma_{r(\theta)}$	Uncertainty budget of ND-RES r electrical (SF of CSP θ thermal) production	[-]
$\eta_{\theta,n}$	Conversion efficiency of thermal to electrical power in segment n of piecewise function of PB of CSP θ	[%]
η_θ	Thermal power output efficiency of CSP θ	[%]
$\eta_\theta^{TS,+(-)}$	Charging (discharging) thermal power efficiency of TS of CSP θ	[%]
Δt	Duration of periods	[hour]
κ	Percentage of reserve traded in the SRM relative to the power capacity of RVPP	[%]
$\lambda_t^{DA}/\lambda_t^{HT}$	DAM/HPA price during period t	[€/MWh]
$\lambda_t^{SR,\uparrow(\downarrow)}$	SRM price for up (down) reserve during period t	[€/MW]
$\hat{\lambda}_t^{SR,\downarrow}/\check{\lambda}_t^{SR,\downarrow}$	Upper bound/negative deviation of the SRM price forecast for down reserve during period t	[€/MW]
$\hat{\lambda}_t^{SR,\uparrow}/\check{\lambda}_t^{SR,\uparrow}$	Upper bound/negative deviation of the SRM price forecast for up reserve during period t	[€/MW]
$\tilde{\lambda}_t^{DA}/\hat{\lambda}_t^{DA}/\check{\lambda}_t^{DA}$	Median value/positive deviation/negative deviation of the DAM price forecast during period t	[€/MWh]
Variables		
$e_{\theta,t}^{TS}$	Thermal energy of TS of CSP θ during period t	[MWh]
h_t^{HT}	Thermal power purchased by RVPP through HPA during period t	[MW]
$h_{\theta,t}$	Thermal power production of CSP θ during period t	[MW]
p_t^{DA}	Electrical power traded by RVPP in the DAM during period t (positive/negative for selling/buying)	[MW]

$p_{\theta,t}^{PB}$	Thermal power of PB of CSP θ during period t	[MW]
$p_{\theta,t}^{SF}$	Thermal power of SF of CSP θ during period t	[MW]
$p_{\theta,t}^{TS,+(-)}$	Thermal charging (discharging) power of TS of CSP θ during period t	[MW]
$p_{d,t}/h_{d,t}$	Electrical/thermal consumption of ED/TD d during period t	[MW]
$p_{r(\theta),t}$	Electrical production of ND-RES r (CSP θ) during period t	[MW]
$r_t^{SR,\uparrow(\downarrow)}$	Up (down) reserve traded by RVPP in the SRM during period t	[MW]
$r_{\theta,t}^{TS,+,\uparrow(\downarrow)}$	Up (down) reserve of TS of CSP θ in the charging state during period t	[MW]
$r_{\theta,t}^{TS,-,\uparrow(\downarrow)}$	Up (down) reserve of TS of CSP θ in the discharging state during period t	[MW]
$r_{\theta,t}^{TS,\uparrow(\downarrow)}$	Up (down) reserve of TS of CSP θ during period t	[MW]
$r_{d,t}^{\uparrow(\downarrow)}$	Up (down) reserve provided by ED d during period t	[MW]
$r_{r(\theta),t}^{\uparrow(\downarrow)}$	Up (down) reserve provided by ND-RES r (CSP θ) during period t	[MW]
$r_{u,t}^{\uparrow(\downarrow)}$	Up (down) reserve provided by RVPP unit u during period t	[MW]
$x_{\theta,n,t}$	Positive variable related to segment n of piecewise function of PB of CSP θ during period t	[-]
y_t^{DA}	Positive auxiliary variable of traded electrical energy in the DAM during period t	[MWh]
$y_{d,t}$	Positive auxiliary variable of ED/TD d consumption uncertainty during period t	[MW]
$y_{r(\theta),t}$	Positive auxiliary variable of ND-RES r electrical (SF of CSP θ thermal) production uncertainty during period t	[MW]
z_t^{DA}	Positive auxiliary variable of DAM electricity price uncertainty during period t	[-]
$z_t^{SR,\uparrow(\downarrow)}$	Positive auxiliary variable of up (down) SRM electricity price uncertainty during period t	[-]
$z_{d,t}$	Positive auxiliary variable of ED/TD d consumption uncertainty during period t	[-]
$z_{r(\theta),t}$	Positive auxiliary variable of ND-RES r electrical (SF of CSP θ thermal) production uncertainty during period t	[-]
ϕ^{DA}	Dual variable to model the DAM price uncertainty	[€]
$\phi^{SR,\uparrow(\downarrow)}$	Dual variable to model the up (down) SRM price uncertainty	[€]
ϕ_d	Dual variable to model the ED/TD d consumption uncertainty	[MW]
$\phi_{r(\theta)}$	Dual variable to model the ND-RES r electrical (SF of CSP θ thermal) production uncertainty	[MW]
$\sigma_\theta^{TS,\uparrow(\downarrow)}$	Share of thermal energy capacity of TS of CSP allocated to provide up (down) reserve	[%]
ζ_t^{DA}	Dual variable to model the DAM price uncertainty during period t	[€]
$\zeta_t^{SR,\uparrow(\downarrow)}$	Dual variable to model the up (down) SRM price uncertainty during period t	[€]
$\zeta_{d,t}$	Dual variable to model the ED/TD d consumption uncertainty during period t	[MW]
$\zeta_{r(\theta),t}$	Dual variable to model the ND-RES r electrical (SF of CSP θ thermal) production uncertainty during period t	[MW]

Binary Variables

$u_{\theta,t}$	Binary variable that is 1 if turbine of CSP θ is online during period t, and 0 otherwise	[-]
$u_{\theta,t}^{TS}$	Binary variable that is 1 if charging state of TS of CSP θ is active, and 0 otherwise	[-]
$v_{\theta,t}^{SU}/v_{\theta,t}^{SD}$	Binary variable that is 1 if turbine of CSP θ starts up/shuts down at period t, and 0 otherwise	[-]
$\chi_{d,t}$	Binary variable that is 1 if ED/TD d consumption worst case occurs during period t, and 0 otherwise	[-]
$\chi_{r(\theta),t}$	Binary variable that is 1 if ND-RES r electrical (SF of CSP θ thermal) power production worst case occurs during period t, and 0 otherwise	[-]

$\varsigma_{\theta,t,n}$	Binary variable that is 1 if segment n of piecewise function of PB of CSP θ is active during period t, and 0 otherwise	[-]

Vectors

$\boldsymbol{\varsigma}_{\theta,t,n} = \{\varsigma^{\uparrow}_{\theta,t,n}, \varsigma^{\downarrow}_{\theta,t,n}, \varsigma_{\theta,t,n}\}$	Vector related to piecewise function of PB of CSP θ for possible reserve activation scenarios	[-]
$\boldsymbol{x}_{\theta,t,n} = \{x^{\uparrow}_{\theta,t,n}, x^{\downarrow}_{\theta,t,n}, x_{\theta,t,n}\}$	Vector related to piecewise function of PB of CSP θ for possible reserve activation scenarios	[-]
$\boldsymbol{r}_{\theta,t} = \{r^{\uparrow}_{\theta,t}, -r^{\downarrow}_{\theta,t}, 0\}$	Vector for possible reserve activation scenarios of CSP θ	[MW]
$\boldsymbol{r}^{TS}_{\theta,t} = \{r^{TS,\uparrow}_{\theta,t}, -r^{TS,\downarrow}_{\theta,t}, 0\}$	Vector for possible reserve activation scenarios of TS of CSP θ	[MW]
$\boldsymbol{r}_{d,t} = \{r^{\uparrow}_{d,t}, -r^{\downarrow}_{d,t}, 0\}$	Vector for possible reserve activation scenarios of ED d	[MW]
$\boldsymbol{r}_{r,t} = \{r^{\uparrow}_{r,t}, -r^{\downarrow}_{r,t}, 0\}$	Vector for possible reserve activation scenarios of ND-RES r	[MW]
$\boldsymbol{r}^{SR}_{t} = \{r^{SR,\uparrow}_{t}, -r^{SR,\downarrow}_{t}, 0\}$	Vector for possible reserve activation scenarios of RVPP	[MW]

1. Introduction

1.1. Motivation

Concentrated Solar Power Plants (CSPs) convert sunlight into heat energy, which can be stored in Thermal Storage (TS), used for electricity generation, or directly applied in heating applications [1, 2]. This thermal energy serves residential uses (e.g., water or space heating, absorption cooling) and industrial processes such as food, chemical, and textile production [3]. Unlike photovoltaics, Parabolic Trough Collector (PTC) mirrors focus sunlight onto a fluid-filled tube that transfers heat to generate steam for turbines. CSPs can store this heat for hours using TS (e.g., molten salt), allowing power generation even after sunset [4]. This enhances their reliability over intermittent sources. CSPs are increasingly applied for industrial decarbonization by supplying renewable process heat. Advances in materials, manufacturing, and design have reduced costs, making CSPs more competitive with other renewables [5]. Large-scale deployment is growing in high-irradiance regions such as Southern Europe, the Middle East, North Africa, Australia, and the United States [6]. With improving storage technologies and falling costs, CSPs are poised for further expansion. Their ability to provide reliable, high-temperature energy makes them well-suited for utility-scale and industrial use [7]. Given their dual ability to generate both thermal and electrical energy—and their flexibility in providing ancillary services like secondary reserve via TS [8]—integrating CSPs into the Renewable-only VPP (RVPP) framework has drawn increasing interest. The RVPP is defined as a set of Renewable Energy Sources (RESs), CSPs, Electric Demands (EDs), and Thermal Demands (TDs) aim of ensuring a safe and reliable operation by offering their combined flexibility (e.g., fast ramp-up/down capability for frequency control), the possibility to internally balance the stochastic RESs fluctuations, and to sell their aggregate generation output in the wholesale market [9].

The primary marketplace for electric energy trading spans the full 24-hour period of the designated day, divided into 24 equal one-hour intervals. This market, known as the Day Ahead Market (DAM), is usually settled 12 hours before the energy delivery period. In this market, generation and demand participants submit selling offers and purchasing bids for each time slot. The Market Operator (MO) then clears the market by evaluating these offers and bids, establishing electricity prices and determining the accepted energy quantities from each participant [10, 11]. In addition to energy markets, Ancillary Service Markets (ASMs) are in place to efficiently allocate resources and ensure the reliable operation of the power system. These markets primarily function by securing predetermined levels of power reserve. Reserve refers to the extra capacity that power plants must allocate in their generation plans to accommodate unforeseen changes in demand or generation shortfalls. The Transmission System Operator (TSO) is tasked with ensuring the

reliability of the power system [12]. The goal of secondary reserve, also known as Automatic Frequency Restoration Reserve (aFRR), is to restore frequency and power exchange to their specified reference values. Any unit aiming to offer aFRR in the market must be certified by the TSO. Key qualifications include the ability to provide reserve for 15 minutes without interruption, within a resolution time of 1 hour, and a response time of 100 seconds [12]. Due to the capabilities of RVPP units—mainly stemming from the flexibility of CSP, and partly from the reserve capacity of flexible EDs and Non-dispatchable Renewable Energy Sources (ND-RES)—RVPP can contribute to secondary reserve and thus participate in the Secondary Reserve Market (SRM) to maximize its profitability. Furthermore, enhancing the heat utilization of CSP can reduce operational costs and increase the efficiency of RVPP [13]. The incorporation of thermal energy trading alongside electrical energy trading can boost the profitability of RVPP [14]. Thermal energy can be traded in various ways: through the thermal energy market [14, 15], locally in the local market [16], or via contracts [17]. Heat Purchase Agreement (HPA) contracts for thermal energy are tailored agreements between two parties, enabling traders to negotiate terms outside a central market or organized exchange [18, 19]. The RVPP can enter into an HPA with a thermal energy service provider to satisfy its remaining TDs. Additionally, the HPA can act as a hedge against market price fluctuations and ensure the fulfillment of TDs when the CSP has low thermal production or is unavailable.

Uncertainty characterization is one of the challenging aspects of RVPP market participation [20, 21]. Uncertainties in the RVPP problem can influence multiple factors, including electricity prices in the DAM and SRM, the thermal output of CSP, the energy production from ND-RES, and the consumption patterns of EDs/TDs [2, 22]. These uncertain parameters can have a substantial effect on the profitability of the RVPP in the market. Thus, addressing this wide range of uncertainties, which characterize the behavior of RVPP units, is crucial for enhancing competitiveness. On one hand, integrating various units into an RVPP can help reduce uncertainties in both production and consumption. As the number of units within the RVPP increases, the likelihood of significant deviations from expected production decreases [9]. Additionally, the CSP can effectively manage uncertainty to maintain the balance between supply and demand within the RVPP [23]. This is made possible by its TS ability to provide energy when other units experience energy fluctuations. However, the RVPP operator must still consider various uncertainties using appropriate optimization techniques. These techniques need to be computationally efficient so that the RVPP can determine its optimal bids and offers before the energy and reserve markets' gate closure or adjust the scheduling of its units accordingly [24]. Furthermore, the RVPP operator must decide on the level of conservatism to apply to different uncertainties and conduct sensitivity analyses, as varying strategies for handling uncertainties can significantly affect profitability [25]. Optimization models should be developed to effectively address the various components of the RVPP problem, including the complexities of different electricity markets, HPA contracts, and inherent uncertainties. Consequently, formulating bidding strategies for RVPP participation across multiple markets—while accounting for the technical characteristics of RVPP units, uncertainty modeling, and market interactions—remains a critical area of focus for both RVPP operators and researchers. This paper provides an in-depth examination of these critical aspects of RVPP market participation.

1.2. Literature Review

The Virtual Power Plant (VPP) scheduling and bidding problem in the electrical energy market, with and without considering different uncertainties, is widely studied in the literature [16, 26–28]. In [16], the optimal bidding strategy of a multi-carrier VPP in energy markets is modeled by a bi-level nonlinear deterministic approach. In [26], the optimal scheduling of a VPP with both renewable and non-renewable energy sources is studied. The scenario-based Stochastic Programming (SP) model is used to capture uncertainties in electricity price, ND-RES production, ED, and TD consumption. The thermal market is adopted to improve the performance of multi-carrier VPP, including RES and combined heat and power units. In [27], an

industrial VPP, including RES, Electrical Storage (ES), and material storage for supplying ED and TD of industrial processes, and financial instruments, is developed. The best and worst-case scenarios of uncertain parameters related to electricity price and ND-RES production are modeled by scenario-based SP, using Value-at-Best (VaB) and Conditional Value-at-Risk (CVaR) criteria, respectively. The paper [28] studies the decision-making of a VPP with energy storage in the DAM and Intra-Day Market (IDM), considering RES uncertainties. The interactions between the VPP, electricity market, and aggregators in the distribution network are taken into account by a rolling horizon optimization technique. These studies predominantly focus on energy market participation, often neglecting ASM, which are critical for maintaining grid stability and reliability. Incorporating ASM participation can provide additional income sources and enhance the operational flexibility and economic performance of VPPs, representing a significant yet underexplored opportunity in these works.

Some papers study different ASMs in addition to energy markets, which can increase the profitability of VPP. The paper [29] examines the peak-regulation ASM participation of a multi-energy VPP, including electrical and thermal units. A two-stage Robust Optimization (RO) is proposed to account for the uncertainties in PV units production and ED and TD consumption. In [30], a model is proposed for multiple technical VPP in the distribution network, allowing for energy trading in the electricity market and energy trading among VPPs. The uncertainties related to RES and ED are considered using a two-stage SP model. The paper [31] proposes a single-level RO approach for RVPP participation in the sequential energy and reserve markets to find the worst-case profit of different uncertainties related to electricity price, ND-RES production, and ED consumption. In [32], this work is extended by incorporating the penalization costs of RVPP in electricity markets using an economic risk analysis approach. Furthermore, carbon trading [33] and thermal energy trading [14, 15] are studied in the VPP optimization problem. In [33], to achieve low-carbon operation of a multi-energy VPP, a carbon trading mechanism is proposed along with DAM participation of VPP. A two-stage Adaptive Robust Optimization (ARO) approach, which is solved by the Column & Constraint Generation (C&CG) algorithm, is proposed to account for the uncertainties related to both the source and load sides. In [14], the optimal scheduling of a multi-energy VPP with several uncertainties in electricity and thermal markets is studied. A two-stage RO-SP approach is implemented to capture the uncertainties of RES production and ED and TD consumption. The paper [15] proposes a multi-objective scheduling of a multi-energy VPP to maximize profit and minimize carbon emissions. Several uncertainties of electricity price, RES production (including PV, Photovoltaic-Thermal (PVT), and Wind Farm (WF)), and ED consumption are taken into account through scenarios. A common limitation of these studies is that they do not consider the joint participation of VPPs in electricity markets, ASMs, and thermal energy trading, thus preventing fully leveraging their operational flexibility and maximizing economic benefits. In addition, while uncertainties related to renewable generation and demand are often considered, price uncertainty in both the energy market and ASMs are typically neglected. Furthermore, the integration of CSP technologies is often overlooked, despite their growing importance in multi-energy VPP systems. These limitations highlight the need for more holistic and realistic modeling approaches to support advanced market participation strategies.

Given the flexibility of CSP through its TS to provide both energy and ancillary services, some papers study CSP independent participation in different markets. In [1], the offering curve of a price-taker CSP in the DAM is obtained. An RO-SP approach is proposed to consider the uncertainties of electricity price and CSP production. In [34], the optimal bidding of CSP in the DAM and Real-time Market (RTM) is investigated. The uncertainties of electricity price and CSP production are modeled by a hybrid stochastic Information Gap Decision Theory (IGDT) approach based on CVaR. The paper in [35] studies the optimal offering strategy of CSP in the DAM energy, reserve market, and regulation markets. The market price uncertainties are considered by scenarios and solar generation uncertainties are modeled by RO. Addition-

ally, some research integrates CSP with WFs [36–39] or biomass plants [40] to improve the performance of power producers in economic dispatch or market participation. In [36], the economic dispatch of CSP with Electric Heaters (EHs) and WFs for the provision of energy and reserve is studied. A two-stage SP model is used to capture the uncertainties of RES. The paper [37] suggests a multi-stage approach for coordinated WF-CSP energy and reserve allocation in the DAM and IDM. The uncertainties of WF and CSP production are taken into account by the ARO approach. In [38], the self-scheduling of WF-CSP power producers in the DAM energy and reserve market is studied. The uncertainties of WF and CSP production are modeled by using the Probability Density Function (PDF) of these uncertain parameters. The paper in [39] studies the bidding approach of CSPs containing EH integrated with WFs for participation in the DAM and ASM. The uncertainties of electricity prices are considered by scenarios, while the uncertainties of CSP and WF production are modeled by stochastic chance-constrained optimization. The paper [40] studies the DAM and IDM dispatch of integrated biomass-CSP by using a multi-objective risk-based approach. A two-stage SP approach for market uncertainties and CVaR-IGDT for CSP uncertainties are used. However, these studies do not adopt a VPP framework and instead consider separate participation of CSP units or their integration with WF or biomass plants, missing the opportunity to fully exploit the operational and economic synergies of diverse assets within a coordinated VPP. Moreover, they focus solely on electricity market participation, neglecting CSP's potential role in thermal energy trading.

Integration of CSP in VPP has been studied in the literature. The paper [41] examines the optimal participation of RVPP including CSP, PV, WF, and hydro plant in the DAM and IDM through a deterministic Mixed Integer Linear Programming (MILP) problem. The paper [42] proposes the deterministic optimal scheduling of CSP-based VPP in the electricity energy and carbon trading markets. The paper [23] suggests a coordinated energy management strategy for WF-CSP integration in multiple VPPs in the DAM. A Distributed RO (DRO) approach using the C&CG algorithm is proposed to capture the uncertainties in CSP and WF production. Despite the work done in this regard, the integration of CSP in VPP, considering multiple uncertainties, electrical and thermal energy markets, and ASM, has not been fully studied in the literature. The paper [25] proposes a flexible RO approach for RVPP participation in electrical markets, including sequential energy and reserve markets. However, thermal energy trading is neglected, and a detailed model for energy conversion is not provided in this paper. In [2], a coordinated strategy for VPP, including CSP, solar PVs, and EDs/TDs, is proposed for scheduling in the DAM and Balancing Market (BAM). SP, through scenario generation and considering CVaR, is used to model various uncertainties in electricity prices, CSP and Photovoltaic (PV) production, and EDs/TDs consumption. The paper [13] proposes a model for the heat utilization of CSP in a VPP composed of integrated Compressed Air Energy Storage (CAES), TS, combined heat and power, and CSP. The uncertainty in solar irradiation and EDs/TDs is addressed by using four scenarios for different seasons. Again, the above two references do not take into account ASM.

Considering the gaps in the literature, this paper investigates the integration of CSP in VPP for the electrical DAM market and ASM (through SRM), along with thermal energy trading via HPA contracts. A two-stage RO approach is developed to account for various uncertainties related to DAM and SRM electricity prices, the electrical production of solar PVs, WFs production, and thermal production of CSP, as well as uncertainties in ED and TD consumption. This work extends the RO framework in [43] by incorporating time-dependent selection of uncertain parameters, allowing for a more practical approach to handling uncertainty on both the source and load sides in VPP market bidding applications. Unlike previous formulations [1, 35, 37], which often define uncertainty sets for each time period, our method integrates temporal considerations into the protection function of uncertain parameters, (the term in the objective function that defines the necessary protection against deviations of uncertain parameters). The procedure for obtaining the refined MILP mathematical formulation from the protection function of uncertainties is also provided. Additionally, for the first time, the reserve provision of CSP is modeled by considering the energy limita-

tion of its TS to guarantee the safe energy and reserve provision of CSP. This is achieved by proposing a mathematical model that assigns an adjustable share of TS exclusively for the provision of reserve. The optimization problem determines the optimal value of the assigned share for reserve provision based on the profitability of the RVPP. Overall, this paper proposes a more comprehensive model for the integration of CSP in RVPP by considering multiple uncertainties and electricity and thermal energy trading options, which is more advanced than existing literature. To support this claim, Table 1 compares the key aspects of the reviewed literature with the proposed approach in this paper.

1.3. Paper Contributions

Considering the research gaps in the literature, the main contributions of this paper are outlined as follows:

- *To consider different markets and contracts to trade electrical and thermal energy for the integration of CSP in RVPP:* This paper models the participation of CSP-based RVPP in the DAM and SRM, and considers the possibility of trading thermal energy through HPA. The participation of RVPP in different combinations of these markets and the use of HPA are presented, and the profitability of RVPP is compared.

- *To develop a refined two-stage RO formulation that considers different uncertainties in the RVPP problem:* In this paper, several uncertainties related to the DAM price, SRM price, ND-RES electrical production, CSP thermal production, and ED and TD consumption are considered using a reformulated two-stage RO model. For the first time, the refined MILP mathematical formulation, incorporating temporal considerations to obtain the worst-case uncertainty for both the source and load sides, is presented.

- *Energy and reserve provision of CSP is modeled by considering the energy limitation of its TS:* The mathematical model in this paper considers an adjustable share of energy from the energy-limited device TS for the provision of up and down reserve. This share of energy is assigned by the optimization problem to maximize RVPP profitability.

- *The proposed two-stage approach for CSP integration in VPP provides high computational efficiency:* Considering several features in the CSP-based RVPP market bidding problem can increase the computational time of the optimization. Some of these features include the number of RVPP units, various uncertainties, trading options, reserve provision, and time-coupling constraints of TS for RVPP. Despite taking into account these features, the proposed MILP two-stage model maintains the computational efficiency, allowing for multiple economic analyses to be performed before determining the final market bid.

2. Problem Description

RVPPs play a key role in integrating ND-RES into electricity markets while reliably meeting ED/TD demand, thus maintaining operational and economic viability. This is achieved by operating its units across multiple markets—such as the DAM and SRM—and by trading thermal energy, while managing uncertainties from market prices, renewable output, and demand. The main challenge is to determine optimal bidding strategies that maximize RVPP profit while ensuring technical feasibility and robustness. Figure 1 presents the structure of the proposed RVPP model, showing its components and optimization framework. The RVPP may include solar PVs, WFs, and CSPs, along with local EDs/TDs. It is connected to the electrical power

9

Table 1: Comparison of proposed approach in this paper and literature.

Ref.	Components				Market (contract)				Uncertainty			VPP concept	Reserve concept	Method & solution
	CSP	RES	Storage	Load	Energy	ASM	Thermal	Price	CSP	RES	Load			
[1]	✓	×	TS	×	DAM	×	×	DAM	✓	×	×	×	×	SP, RO
[2]	✓	PV	TS	ED/TD	DAM/BAM	×	×	DAM/BAM	✓	PV	ED/TD	✓	×	SP, CVaR
[13]	✓	×	ES/TS	ED/TD	DAM	×	Thermal	×	✓	×	ED/TD	✓	×	Scenario-based, MILP
[14]	×	PV/WF	ES/TS	ED/TD	DAM	×	Thermal	×	×	PV/WF	ED/TD	✓	×	Two-stage RO-SP, C&CG
[15]	×	PV/PVT/WF	ES/TS	ED/TD	DAM	Reserve	Thermal	DAM	×	PV/PVT/WF	ED	✓	Spinning reserve	Scenario-based SP, Fuzzy
[16]	×	PV/WF	×	ED/TD	DAM	×	Thermal	×	×	×	×	✓	×	Deterministic, Bi-level, Nonlinear
[23]	✓	WF	ES/TS	ED	DAM	×	×	×	✓	WF	×	✓	×	DRO, C&CG
[25]	✓	PV/WF	×	ED	DAM/IDM	SRM	×	DAM/IDM/SRM	✓	PV/WF	ED	✓	Up/down reserve	RO, MILP
[26]	×	PV/PVT/WF	ES	ED/TD	DAM	×	×	DAM	×	PV/PVT/WF	ED/TD	✓	×	Scenario-based SP, MILP
[27]	×	WF	ES	ED/TD	DAM/RTM	×	×	DAM/RTM	×	WF	×	✓	×	Scenario-based SP, CVaR, VaB
[28]	×	PV/WF	ES/TS	ED/TD	DAM/IDM	×	×	×	×	PV/WF	×	✓	×	Rolling horizon, Nonlinear
[29]	×	PV	ES/TS	ED/TD	DAM	Peak regulation	×	×	×	PV	ED/TD	✓	×	Two-stage RO, C&CG
[30]	×	PV/WF	ES	ED	DAM	Congestion management	×	×	×	PV/WF	ED	✓	×	Two-stage SP, MILP
[31]	×	PV/WF	×	ED	DAM	SRM	×	DAM/SRM	×	PV/WF	ED	✓	Up/down reserve	RO, MILP
[33]	×	PV/WF	ES	ED/TD	DAM	×	×	×	×	PV/WF	ED/TD	✓	×	Two-stage ARO, C&CG
[34]	✓	×	TS	×	DAM/RTM	×	×	DAM/RTM	✓	×	×	×	×	SP-IGDT, CVaR
[35]	✓	×	TS	×	DAM	Reserve, Regulation	×	DAM/ASM	✓	×	×	×	Responsive reserve, Regulation up/down	SP, RO
[36]	✓	WF	TS	×	×	×	×	×	✓	WF	×	×	Reserve scheduling	Two-stage SP
[37]	✓	WF	TS	×	DAM/IDM	×	×	×	✓	×	×	×	Reserve scheduling	Multi-stage ARO
[38]	✓	WF	TS	×	DAM	Reserve	×	×	✓	WF	×	×	Spinning reserve	PDF, MILP
[39]	✓	WF	TS	×	DAM	Reserve, Regulation	×	DAM/ASM	✓	WF	×	×	Responsive reserve, Regulation up/down	SP,
[40]	✓	Biomass	TS	×	DAM/IDM	×	×	DAM/IDM	✓	×	×	×	×	Chance constrained Two-stage SP, CVaR-IGDT
[41]	✓	PV/WF/Hydro	TS	ED	DAM/IDM	×	×	×	✓	×	×	✓	×	Deterministic, MILP
[42]	✓	PV/WF	ES	ED/TD	DAM	×	×	×	✓	×	×	✓	×	Master-slave game
This paper	✓	PV/WF	TS	ED/TD	DAM	SRM	HPA contract	DAM/SRM	✓	PV/WF	ED/TD	✓	Up/down reserve, TS reserve allocation	Two-stage RO, MILP

network to trade electricity in the DAM and sell reserves in the SRM. RVPP thermal demand can be met locally by the CSP or externally via the HPA, which offers fixed time-based pricing [18], helping hedge against price fluctuations.

The electricity MO is responsible for clearing the DAM based on the offers and bids submitted by the RVPP and other participants in the electricity markets [10]. The TSO assigns the required secondary reserve according to the security economic dispatch to maintain network security. Additionally, the TSO and MO determine the final accepted reserve offers in the SRM to ensure that sufficient reserves are available to manage real-time imbalances [12]. It is assumed that the RVPP is a price taker in the market, offering electricity at zero price in the DAM and SRM and bidding at a high price for purchasing electricity. This approach increases the likelihood of the RVPP's offers and bids being accepted. Since all RVPP units are renewable, with zero production costs and low operational costs, and given that the RVPP is relatively small compared to the overall network, this assumption is reasonable and aligns with the integration of renewable resources into the grid.

The RVPP forecast center analyzes historical data on key uncertain parameters—including DAM/SRM prices, the output of WFs, PVs, and the Solar Field (SF) of CSP, and the consumption of EDs/TDs—to determine forecast bounds. These bounds are passed to the RVPP data center. The RVPP operator uses forecasted prices, generation, load, and technical data to manage energy flows by solving the proposed optimization problem. The goal is to maximize the value of electricity and reserve trading in the DAM and SRM, while accounting for HPA thermal energy costs and the operational costs of ND-RESs and CSPs. Deterministic constraints govern production, consumption, and energy balances, while uncertain constraints cover generation from ND-RESs/CSPs and load forecasts. Price uncertainty in the objective function is modeled using additional constraints.

Since uncertain parameters can negatively impact the objective function of the RVPP operator, a two-stage RO model is used to account for their effects in the optimization problem [29]. The first stage aims to maximize the benefits of the RVPP, while the second stage considers the flexible worst cases of uncertain parameters. The flexibility of the two-stage RO model is achieved by introducing an input parameter called the *uncertainty budget* for each source of uncertainty [43]. This parameter determines the number of hours within the entire time period during which uncertain parameters deviate to their worst-case values. Therefore, the RVPP operator can adjust the required protection against uncertainty by modifying this parameter. After solving the optimization problem, the RVPP operator provides the internal dispatch of its units, the offers/bids for electrical energy and reserve in the DAM and SRM, as well as the amount of thermal energy purchased through the HPA, to the RVPP data center. This information is then transmitted to the relevant entities, including RVPP units, MO and TSO, and the thermal energy service provider.

3. Two-stage Robust Optimization Problem Formulation

To effectively manage the participation of the RVPP in both electricity and reserve markets, as well as the assignment of thermal energy through HPA contracts, a comprehensive mathematical formulation is required. The optimization framework must account for the technical characteristics of the units, market mechanisms, and multiple sources of uncertainty. The two-stage RO approach effectively captures uncertainty by structuring decisions into two sequential stages: the first stage determines the RVPP's initial market bids and operational plans, while the second stage adjusts to the flexible worst-case realization of uncertain parameters, ensuring that the solution remains feasible and robust against adverse conditions [29]. Therefore, this section develops a two-stage RO optimization framework to model the RVPP's decision-making process under uncertainty, aiming to maximize its profitability while satisfying operational and market constraints. The deterministic formulation by considering a single value for different uncertain parameters is
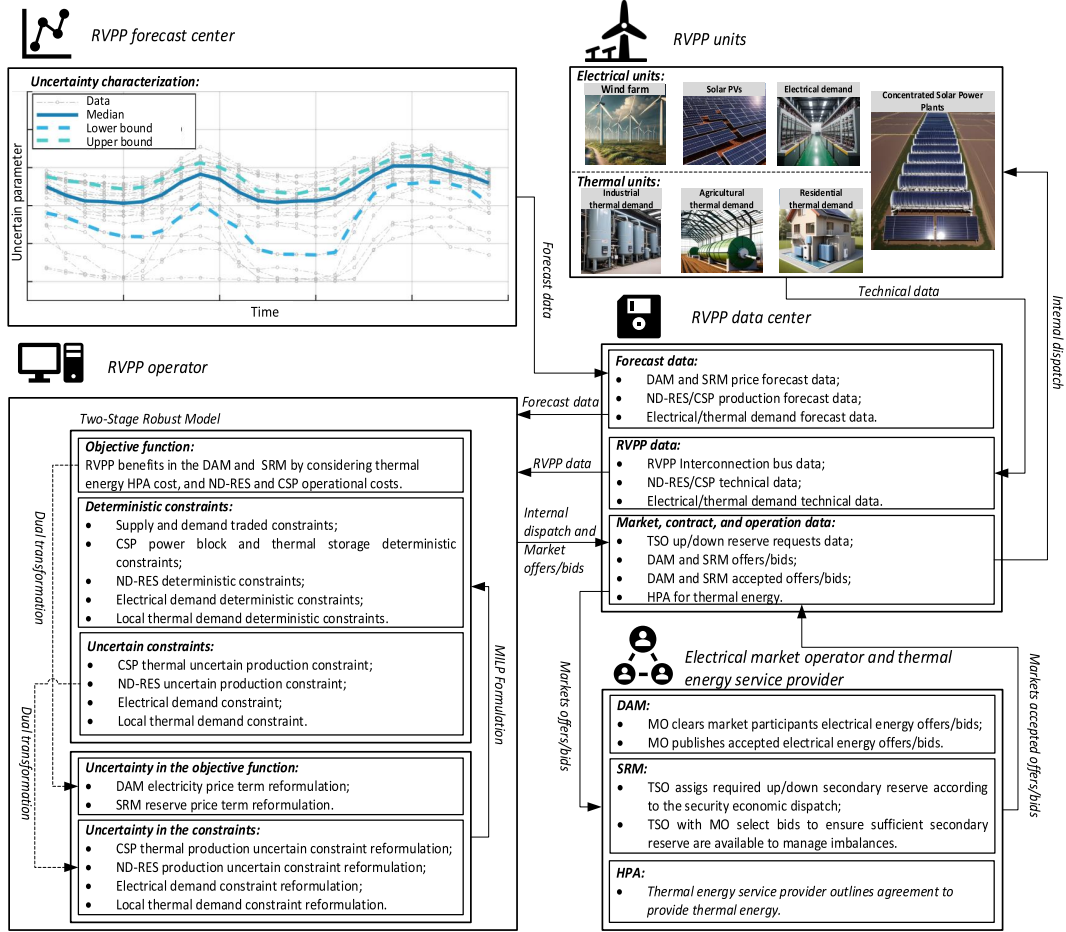
Figure 1: The scheme of considered RVPP for participation in electricity markets, as well as the establishment of HPA contracts.

presented in Section 3.1. The two-stage robust approach to take into account different uncertainties in the objective function and constraints of optimization problem is provided in Section 3.2.

3.1. Deterministic Formulation

The deterministic formulation accounts for the operation and bidding of the RVPP in the electrical energy and reserve markets, assuming the *exact* value of uncertain parameters. This section presents the deterministic objective function and constraints of the optimization problem.

3.1.1. Objective Function

The deterministic objective function, outlined in (1), aims to maximize the RVPP's benefits in the electrical DAM and SRM, while accounting for thermal energy HPA costs. The first term of (1) represents the

expected revenues from the RVPP's bids in the DAM, as well as upward and downward SRM. The second term accounts for the expected costs from purchasing thermal energy through the HPA, while the third and fourth terms calculate the operational costs associated with ND-RESs and CSPs.

$$
\max_{\Xi^{DA+SR+HPA}} \sum_{t \in \mathcal{T}} \left[\lambda_t^{DA} p_t^{DA} \Delta t + \lambda_t^{SR,\uparrow} r_t^{SR,\uparrow} + \lambda_t^{SR,\downarrow} r_t^{SR,\downarrow} \right] - \sum_{t \in \mathcal{T}} \lambda_t^{HT} h_t^{HT} \Delta t
$$

$$
- \sum_{t \in \mathcal{T}} \sum_{r \in \mathcal{R}} C_r p_{r,t} \Delta t - \sum_{t \in \mathcal{T}} \sum_{\theta \in \Theta} C_\theta (p_{\theta,t} + h_{\theta,t}) \Delta t \tag{1}
$$

3.1.2. Supply & Demand Traded Constraints

The equality constraint governing the supply-demand balance of electrical energy and reserve for RVPP units is defined in (2a). This accounts for all possible reserve activation scenarios in real-time, including upward reserve activation, downward reserve activation, and no reserve activation. To model these scenarios, vectors $\boldsymbol{r}_t^{SR} = \{r_t^{SR,\uparrow}, -r_t^{SR,\downarrow}, 0\}$; $\boldsymbol{r}_{r,t} = \{r_{r,t}^{\uparrow}, -r_{r,t}^{\downarrow}, 0\}$; $\boldsymbol{r}_{\theta,t} = \{r_{\theta,t}^{\uparrow}, -r_{\theta,t}^{\downarrow}, 0\}$; and $\boldsymbol{r}_{d,t} = \{r_{d,t}^{\uparrow}, -r_{d,t}^{\downarrow}, 0\}$ are defined for RVPP, ND-RES, CSP, and ED/TD. Hence, (2a) conforms a set of three equations. Equation (2b) defines the equality constraint for thermal energy, where the heat generated by the CSP, along with the thermal energy purchased through the HPA, meets the demand. The upper and lower bounds for the total electrical energy and reserve traded by the RVPP are governed by equations (2c) and (2d), respectively. The traded up and down reserve of the RVPP is limited to a proportion of its maximum electrical production minus its EDs capacity, as outlined in constraints (2e) and (2f) [25].

$$
\sum_{r \in \mathcal{R}} [p_{r,t} + \boldsymbol{r}_{r,t}] + \sum_{\theta \in \Theta} [p_{\theta,t} + \boldsymbol{r}_{\theta,t}] - \sum_{d \in \mathcal{D}} [p_{d,t} - \boldsymbol{r}_{d,t}] = p_t^{DA} + \boldsymbol{r}_t^{SR} ; \qquad \forall t \in \mathcal{T} \tag{2a}
$$

$$
\sum_{\theta \in \Theta} h_{\theta,t} + h_t^{HT} = \sum_{d \in \mathcal{D}} h_{d,t} ; \qquad \forall t \in \mathcal{T} \tag{2b}
$$

$$
p_t^{DA} + r_t^{SR,\uparrow} \leq \sum_{r \in \mathcal{R}} \bar{P}_r + \sum_{\theta \in \Theta} \bar{P}_\theta ; \qquad \forall t \in \mathcal{T} \tag{2c}
$$

$$
- \sum_{d \in \mathcal{D}} \bar{P}_d \leq p_t^{DA} - r_t^{SR,\downarrow} ; \qquad \forall t \in \mathcal{T} \tag{2d}
$$

$$
r_t^{SR,\uparrow} \leq \kappa \left(\sum_{r \in \mathcal{R}} \bar{P}_r + \sum_{\theta \in \Theta} \bar{P}_\theta - \sum_{d \in \mathcal{D}} \bar{P}_d \right) ; \qquad \forall t \in \mathcal{T} \tag{2e}
$$

$$
r_t^{SR,\downarrow} \leq \kappa \left(\sum_{r \in \mathcal{R}} \bar{P}_r + \sum_{\theta \in \Theta} \bar{P}_\theta - \sum_{d \in \mathcal{D}} \bar{P}_d \right) ; \qquad \forall t \in \mathcal{T} \tag{2f}
$$

3.1.3. Concentrated Solar Power Plant

CSPs are synchronous power plants that harness sunlight to produce thermal energy, which can be utilized for electricity generation, residential heating, or industrial applications. PTCs consist of long, curved mirrors that concentrate sunlight onto a tube containing a heat-transfer fluid, which absorbs the heat and facilitates energy transfer in the SF. The conversion of thermal energy into electrical power occurs in the Power Block (PB) of the CSP, where steam generated by the heated fluid drives a turbine. Additionally, molten salt TS enable CSP to store heat for several hours, allowing for electricity production or heat supply even after sunset [4]. As a note, the TS can only be charged if energy is available at the SF, i.e., it cannot be charged
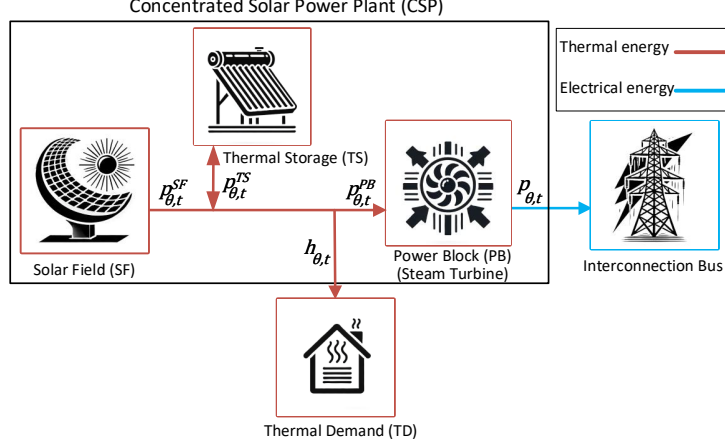
Figure 2: Scheme of the CSP providing electrical and thermal energy.

by consuming (*purchasing*) energy from the grid. Figure 2 illustrates the CSP configuration proposed in this paper, which can deliver both electricity (including energy and reserve) and thermal energy. Compared to ND-RESs, CSPs introduce additional complexities in uncertainty modeling, as solar resource variability affects thermal energy production within the SF. Furthermore, the conversion process from thermal to electrical energy requires explicit modeling while considering reserve provision. Additionally, the presence of TS adds further complexity due to the need to account for different states of charging and discharging. The model must ensure that reserve provision does not compromise the availability of stored energy in the TS for later use. These interdependencies make the modeling of CSPs significantly more intricate than that of ND-RES assets.

A. CSP Power Block Constraints

The formulation for converting thermal energy into electrical energy in the PB of the CSP, with explicit consideration of reserve provision, is provided in (3) [9]. This set of constraints models the interactions between the thermal subsystem (SF, TS, and turbine) and the electrical output. Specifically, constraint (3a) defines the operational bounds of the thermal power output from the SF, which depend on a fixed realization of the uncertain SF power ($P_{\theta,t}^{SF}$). Constraint (3b) captures the core thermal power balance feeding into the PB, linking it to several components, as illustrated in Figure 2. These components include the thermal power supplied by the SF ($p_{\theta,t}^{SF}$), the charging and discharging power of the TS ($p_{\theta,t}^{TS,+}$ and $p_{\theta,t}^{TS,-}$), the thermal power allocated to local TDs ($h_{\theta,t}$), adjusted by the efficiency of thermal energy provision to TDs (η_θ), and the thermal losses associated with turbine startup (K_θ^{PB}). This constraint demonstrates the first key coupling between thermal inflows and their effect on the net thermal energy available for electricity generation. The thermal power and reserve supplied to the PB of the CSP are constrained by the PB's upper and lower power capacity ($\bar{P}_\theta^{PB}$ and $\underline{P}_\theta^{PB}$) and the turbine's commitment status, represented by the binary variable $u_{\theta,t}$, as outlined in (3c)–(3d). These bounds ensure that the turbine's operation aligns with its physical limitations and operational status. The commitment status of the PB and its associated constraints, including the minimum up/down time requirements, are detailed in the supplementary constraints provided in Appendix A. The electrical power ($p_{\theta,t}$) and reserve output ($r_{\theta,t}$) from the PB are calculated in (3e), which uses a piecewise linear function to model thermal-to-electric conversion efficiency. If the total thermal power and

reserve ($p_{\theta,t}^{PB} + r_{\theta,t}^{TS}$) injected into the PB falls below a specified threshold, the turbine cannot turn on, resulting in zero output, as defined by the first term on the right-hand side of (3e). Once the injected thermal energy exceeds this threshold, the turbine begins generating electricity according to the piecewise linear segments represented by the second term on the right-hand side of (3e). The efficiency $\eta_{\theta,n}$ of each segment in the piecewise linear function varies based on the thermal power and reserve injected into the PB. The real-time reserve activation scenarios for the TS, encompassing upward reserve activation, downward reserve activation, and no reserve activation, are represented by the vector $\boldsymbol{r}_{\theta,t}^{TS} = \{r_{\theta,t}^{TS,\uparrow}, -r_{\theta,t}^{TS,\downarrow}, 0\}$. The vector $\boldsymbol{r}_{\theta,t} = \{r_{\theta,t}^{\uparrow}, -r_{\theta,t}^{\downarrow}, 0\}$ represents the different states of reserve activation for the final reserve supplied by the CSP (see (2a)). This formulation illustrates the second major thermal-electrical coupling, where thermal reserve activation directly impacts potential electrical reserve output. Constraints (3f)–(3g) set upper limits on the electrical upward and downward reserves ($r_{\theta,t}^{\uparrow}$ and $r_{\theta,t}^{\downarrow}$) the CSP can supply to the system. Finally, the binary nature of the turbine commitment variables $u_{\theta,t}$ and $v_{\theta,t}^{SU}$ is enforced in (3h), supporting the logical consistency of thermal operation states. Collectively, the set of constraints (3) ensures that the thermal decision variables—whether related to thermal power or reserve—are internally consistent with the electrical output and market participation framework, thereby establishing a valid thermal-electrical coupling within the model.

$$0 \le p_{\theta,t}^{SF} \le P_{\theta,t}^{SF} ; \qquad\qquad\qquad \forall \theta, t \in \Theta, \mathcal{T} \quad (3a)$$

$$p_{\theta,t}^{PB} = p_{\theta,t}^{SF} - \frac{h_{\theta,t}}{\eta_\theta} + p_{\theta,t}^{TS,-} - p_{\theta,t}^{TS,+} - K_\theta^{PB} v_{\theta,t}^{SU} \bar{P}_\theta^{PB} ; \qquad\qquad \forall \theta, t \in \Theta, \mathcal{T} \quad (3b)$$

$$p_{\theta,t}^{PB} + r_{\theta,t}^{TS,\uparrow} \le \bar{P}_\theta^{PB} u_{\theta,t} ; \qquad\qquad\qquad \forall \theta, t \in \Theta, \mathcal{T} \quad (3c)$$

$$\underline{P}_\theta^{PB} u_{\theta,t} \le p_{\theta,t}^{PB} - r_{\theta,t}^{TS,\downarrow} ; \qquad\qquad\qquad \forall \theta, t \in \Theta, \mathcal{T} \quad (3d)$$

$$p_{\theta,t} + \boldsymbol{r}_{\theta,t} = \begin{cases} 0, & if \quad 0 \le p_{\theta,t}^{PB} + \boldsymbol{r}_{\theta,t}^{TS} \le P_{\theta,n=1}^{PB} ; & \forall \theta, t \in \Theta, \mathcal{T} \\ \eta_{\theta,n}(p_{\theta,t}^{PB} + \boldsymbol{r}_{\theta,t}^{TS}), & if \quad P_{\theta,n-1}^{PB} \le p_{\theta,t}^{PB} + \boldsymbol{r}_{\theta,t}^{TS} \le P_{\theta,n}^{PB} ; & \forall \theta, t, n \in \Theta, \mathcal{T}, \mathcal{N}, n \backslash \{0,1\} \end{cases} \quad (3e)$$

$$r_{\theta,t}^{\uparrow} \le T^{SR} \bar{R}_\theta^{SR} ; \qquad\qquad\qquad \forall \theta, t \in \Theta, \mathcal{T} \quad (3f)$$

$$r_{\theta,t}^{\downarrow} \le T^{SR} \underline{R}_\theta^{SR} ; \qquad\qquad\qquad \forall \theta, t \in \Theta, \mathcal{T} \quad (3g)$$

$$u_{\theta,t}, v_{\theta,t}^{SU} \in \{0,1\} ; \qquad\qquad\qquad \forall \theta, t \in \Theta, \mathcal{T} \quad (3h)$$

The conditional piecewise function in (3e) must be reformulated as a set of linear constraints to ensure compatibility with the MILP programming framework. To achieve this, Special Ordered Set of type 2 (SOS-2) constraints are introduced in (4), which allow the piecewise linear relationship to be modeled accurately and efficiently within the optimization problem. Constraint (4a) ensures that the input thermal power and reserve variables lie within the breakpoints of each piecewise segment of the PB, thereby defining the convex combination of these breakpoints. Constraint (4b) defines the output electrical power and reserve variables as weighted sums of the corresponding efficiencies and breakpoints. Constraints (4c)–(4f) enforce the SOS-2 property, guaranteeing that only two adjacent breakpoints can have positive weights at any time, which preserves the piecewise linearity and ensures solution feasibility. The vectors $\boldsymbol{x}_{\theta,t,n} = \{x_{\theta,t,n}^{\uparrow}, x_{\theta,t,n}^{\downarrow}, x_{\theta,t,n}\}$ and $\boldsymbol{\varsigma}_{\theta,t,n} = \{\varsigma_{\theta,t,n}^{\uparrow}, \varsigma_{\theta,t,n}^{\downarrow}, \varsigma_{\theta,t,n}\}$ represent variables associated with the different reserve activation scenarios. Finally, constraints (4g) and (4h) define the nature of the continuous and binary variables, respectively,

ensuring the correct formulation of the SOS-2 structure.

$$p_{\theta,t}^{PB} + \boldsymbol{r}_{\theta,t}^{TS} = \sum_{n\in\mathcal{N}} P_{\theta,n}^{PB}\boldsymbol{x}_{\theta,t,n} \;; \qquad\qquad \forall\theta, t \in \Theta, \mathcal{T} \qquad\qquad (4a)$$

$$p_{\theta,t} + \boldsymbol{r}_{\theta,t} = \sum_{n\in\mathcal{N}} \eta_{\theta,n} P_{\theta,n}^{PB}\boldsymbol{x}_{\theta,t,n} \;; \qquad\qquad \forall\theta, t \in \Theta, \mathcal{T} \qquad\qquad (4b)$$

$$\sum_{n\in\mathcal{N}} \boldsymbol{x}_{\theta,t,n} = 1 \;; \qquad\qquad \forall\theta, t \in \Theta, \mathcal{T} \qquad\qquad (4c)$$

$$\sum_{n\in\mathcal{N}} \boldsymbol{\varsigma}_{\theta,t,n} \le 2 \;; \qquad\qquad \forall\theta, t \in \Theta, \mathcal{T} \qquad\qquad (4d)$$

$$\boldsymbol{x}_{\theta,t,n} \le \boldsymbol{\varsigma}_{\theta,t,n} \;; \qquad\qquad \forall\theta, t, n \in \Theta, \mathcal{T}, \mathcal{N} \qquad\qquad (4e)$$

$$\boldsymbol{\varsigma}_{\theta,t,n} + \boldsymbol{\varsigma}_{\theta,t,n'} \le 1 \;; \qquad \forall\theta, t, n \in \Theta, \mathcal{T}, \mathcal{N}, n \le |\mathcal{N}| - 3, n' \ge n + 2 \qquad\qquad (4f)$$

$$\boldsymbol{x}_{\theta,t,n} \ge 0 \;; \qquad\qquad \forall\theta, t, n \in \Theta, \mathcal{T}, \mathcal{N} \qquad\qquad (4g)$$

$$\boldsymbol{\varsigma}_{\theta,t,n} \in \{0, 1\} \;; \qquad\qquad \forall\theta, t, n \in \Theta, \mathcal{T}, \mathcal{N} \qquad\qquad (4h)$$

B. CSP Thermal Storage Constraints

The TS system of the CSP unit is modeled to simultaneously support both thermal energy delivery and reserve provision, using a set of operational and energy balance constraints defined in (5). To mitigate potential infeasibility issues in the operation of the TS, the model—based on the approach in [9]—allocates a specific portion of the TS's energy capacity exclusively for upward (↑) and downward (↓) reserve provision. Constraints (5a)-(5d) define the operational bounds for thermal charging (+) and discharging (−), while incorporating the corresponding upward and downward reserve contributions. The TS can operate in only one mode at a time—either charging (storing thermal energy) or discharging (release stored energy)—as enforced by the binary variable $u_{\theta,t}^{TS}$, which takes the value 1 for charging and 0 for discharging. Specifically, constraints (5a)-(5b) define the allowable charging power range $p_{\theta,t}^{TS,+}$, adjusted for the upward or downward reserve allocated during charging (i.e., $r_{\theta,t}^{TS,+,\uparrow}$, $r_{\theta,t}^{TS,+,\downarrow}$). Similarly, constraints (5c)-(5d) define limits for discharging power $p_{\theta,t}^{TS,-}$, accounted for both upward and downward reserve provision in that mode (i.e., $r_{\theta,t}^{TS,-,\uparrow}$, $r_{\theta,t}^{TS,-,\downarrow}$). These constraints ensure that the TS does not exceed its power capacity limits during either mode of operation, even when reserves are provided. Because the TS may contribute reserves in both charging and discharging states, the total upward and downward reserves $r_{\theta,t}^{TS,\uparrow}$ and $r_{\theta,t}^{TS,\downarrow}$ are expressed as the sum of the contributions from both modes. Constraint (5e) shows that total upward reserve is the sum of reserve available during discharging and charging. Constraint (5f) is similarly presented for provided total downward reserve by TS. This flexible formulation allows the TS to participate in reserve ancillary services regardless of its charging state, enhancing its system value. Constraints (5g)–(5h) ensure thermal energy balance and proper cycling within the storage tank. Constraint (5g) captures the energy balance over time, where the energy level is updated based on the charging power ($p_{\theta,t}^{TS,+}$), discharging power ($p_{\theta,t}^{TS,-}$), their respective efficiencies ($\eta_{\theta}^{TS,+}$ and $\eta_{\theta}^{TS,-}$), and the time step size (Δt). To complement (5g), equation (5h) ensures that the state of charge is equal at the initial and final periods. This constraint is relevant for DAM operation and scheduling of representative periods, as it maintains the TS energy level at the same state at the start of each cycle, avoiding any bias in the schedule caused by depleting or overfilling the tank near the end of the horizon. To prevent conflicts between energy commitments and reserve activation, a share of the thermal energy capacity is explicitly reserved. Constraints (5i) and (5j) limit the total energy that can be used

16

for upward and downward reserve over the horizon to a fraction of the usable capacity. These fractions are represented by the variables $\sigma_\theta^{TS,\uparrow}$ and $\sigma_\theta^{TS,\downarrow}$, and they prevent overcommitting reserves without sufficient energy backup. Based on the energy allocated for reserve provision, the operational energy limits of the TS are established in (5k), ensuring that energy allocated for reserves remains available by effectively separating energy used for power and reserve. Finally, constraint (5l) enforces the binary nature of the operating mode variable $u_{\theta,t}^{TS}$, which is essential to ensure mutually exclusive charging and discharging states.

$$\underline{P}_\theta^{TS,+} u_{\theta,t}^{TS} \le p_{\theta,t}^{TS,+} - r_{\theta,t}^{TS,+,\uparrow} \; ; \qquad\qquad \forall \theta, t \in \Theta, \mathcal{T} \qquad (5a)$$

$$p_{\theta,t}^{TS,+} + r_{\theta,t}^{TS,+,\downarrow} \le \bar{P}_\theta^{TS,+} u_{\theta,t}^{TS} \; ; \qquad\qquad \forall \theta, t \in \Theta, \mathcal{T} \qquad (5b)$$

$$p_{\theta,t}^{TS,-} + r_{\theta,t}^{TS,-,\uparrow} \le \bar{P}_\theta^{TS,-} \left(1 - u_{\theta,t}^{TS} \right) \; ; \qquad\qquad \forall \theta, t \in \Theta, \mathcal{T} \qquad (5c)$$

$$\underline{P}_\theta^{TS,-} \left(1 - u_{\theta,t}^{TS} \right) \le p_{\theta,t}^{TS,-} - r_{\theta,t}^{TS,-,\downarrow} \; ; \qquad\qquad \forall \theta, t \in \Theta, \mathcal{T} \qquad (5d)$$

$$r_{\theta,t}^{TS,\uparrow} = r_{\theta,t}^{TS,+,\uparrow} + r_{\theta,t}^{TS,-,\uparrow} \; ; \qquad\qquad \forall \theta, t \in \Theta, \mathcal{T} \qquad (5e)$$

$$r_{\theta,t}^{TS,\downarrow} = r_{\theta,t}^{TS,+,\downarrow} + r_{\theta,t}^{TS,-,\downarrow} \; ; \qquad\qquad \forall \theta, t \in \Theta, \mathcal{T} \qquad (5f)$$

$$e_{\theta,t}^{TS} = e_{\theta,t-1}^{TS} + p_{\theta,t}^{TS,+} \eta_\theta^{TS,+} \Delta t - \frac{p_{\theta,t}^{TS,-} \Delta t}{\eta_\theta^{TS,-}} \; ; \qquad\qquad \forall \theta, t \in \Theta, \mathcal{T}, t\backslash\{1\} \qquad (5g)$$

$$e_{\theta,1}^{TS} = e_{\theta,t=T}^{TS} \; ; \qquad\qquad \forall \theta \in \Theta \qquad (5h)$$

$$\sum_{t \in \mathcal{T}} \frac{r_{\theta,t}^{TS,\uparrow} \Delta t}{\eta_\theta^{TS,-}} \le \sigma_\theta^{TS,\uparrow} \left(\bar{E}_\theta^{TS} - \underline{E}_\theta^{TS} \right) \; ; \qquad\qquad \forall \theta \in \Theta \qquad (5i)$$

$$\sum_{t \in \mathcal{T}} r_{\theta,t}^{TS,\downarrow} \eta_\theta^{TS,+} \Delta t \le \sigma_\theta^{TS,\downarrow} \left(\bar{E}_\theta^{TS} - \underline{E}_\theta^{TS} \right) \; ; \qquad\qquad \forall \theta \in \Theta \qquad (5j)$$

$$\underline{E}_\theta^{TS} + \sigma_\theta^{TS,\downarrow} \left(\bar{E}_\theta^{TS} - \underline{E}_\theta^{TS} \right) \le e_{\theta,t}^{TS} \le \bar{E}_\theta^{TS} - \sigma_\theta^{TS,\downarrow} \left(\bar{E}_\theta^{TS} - \underline{E}_\theta^{TS} \right) \; ; \qquad\qquad \forall \theta, t \in \Theta, \mathcal{T} \qquad (5k)$$

$$u_{\theta,t}^{TS} \in \{0, 1\} \; ; \qquad\qquad \forall \theta, t \in \Theta, \mathcal{T} \qquad (5l)$$

3.1.4. ND-RES Constraints

The constraints related to ND-RESs are formulated in (6). The upper and lower bounds for the output energy and reserve of ND-RESs, using the precise value for the uncertain parameter, are defined in constraints (6a) and (6b), respectively. It is important to highlight that ND-RESs, such as WFs and solar PVs, have the potential to provide reserve in the SRM, subject to their technical capabilities [44, 45]. Upward reserve can be supplied when ND-RESs are operated at a curtailed level and then increase their generation during reserve activation. In contrast, downward reserve is provided by reducing their output power from the existing operational level. The up and down reserve provision capabilities by ND-RESs are constrained by equations (6c) and (6d), respectively.

$$p_{r,t} + r_{r,t}^{\uparrow} \le P_{r,t} \; ; \qquad\qquad \forall r, t \in \mathcal{R}, \mathcal{T} \qquad (6a)$$

$$\underline{P}_r \le p_{r,t} - r_{r,t}^{\downarrow} \; ; \qquad\qquad \forall r, t \in \mathcal{R}, \mathcal{T} \qquad (6b)$$

$$r_{r,t}^{\uparrow} \le T^{SR} \underline{R}_r^{SR} \; ; \qquad\qquad \forall r, t \in \mathcal{R}, \mathcal{T} \qquad (6c)$$

$$r_{r,t}^{\downarrow} \le T^{SR} \bar{R}_r^{SR} \; ; \qquad\qquad \forall r, t \in \mathcal{R}, \mathcal{T} \qquad (6d)$$

17

3.1.5. Demand Constraints

The constraints for flexible EDs and local TDs are provided in (7). Constraints (7a) and (7b) set fixed values for the uncertainties associated with EDs/TDs, respectively. The lower and upper bounds for flexible EDs, considering reserve provision, are defined in (7c) and (7d), respectively. The bound for TDs are determined by the capacity of the thermal pipe connected to the demand, as specified in (7e). In this study, EDs are allowed a certain percentage of flexibility relative to its predefined profile, which is allocated for up and down reserve provision according to (7f) and (7g), respectively [46]. The up and down reserves provided by EDs are further constrained by the demand's ability to provide reserve, as specified in (7h) and (7i). Additionally, the minimum energy consumption over the time horizon for both EDs/TDs is constrained by (7j) and (7k), respectively.

$$p_{d,t} \geq P_{d,t} \; ; \qquad\qquad \forall d, t \in \mathcal{D}, \mathcal{T} \qquad (7a)$$

$$h_{d,t} \geq H_{d,t} \; ; \qquad\qquad \forall d, t \in \mathcal{D}, \mathcal{T} \qquad (7b)$$

$$\underline{P}_d \leq p_{d,t} - r^{\uparrow}_{d,t} \; ; \qquad\qquad \forall d, t \in \mathcal{D}, \mathcal{T} \qquad (7c)$$

$$p_{d,t} + r^{\downarrow}_{d,t} \leq \bar{P}_d \; ; \qquad\qquad \forall d, t \in \mathcal{D}, \mathcal{T} \qquad (7d)$$

$$h_{d,t} \leq \bar{H}_d \; ; \qquad\qquad \forall d, t \in \mathcal{D}, \mathcal{T} \qquad (7e)$$

$$r^{\uparrow}_{d,t} \leq \underline{\beta}_{d,t} p_{d,t} \; ; \qquad\qquad \forall d, t \in \mathcal{D}, \mathcal{T} \qquad (7f)$$

$$r^{\downarrow}_{d,t} \leq \bar{\beta}_{d,t} p_{d,t} \; ; \qquad\qquad \forall d, t \in \mathcal{D}, \mathcal{T} \qquad (7g)$$

$$r^{\uparrow}_{d,t} \leq T^{SR} \underline{R}^{SR}_d \; ; \qquad\qquad \forall d, t \in \mathcal{D}, \mathcal{T} \qquad (7h)$$

$$r^{\downarrow}_{d,t} \leq T^{SR} \bar{R}^{SR}_d \; ; \qquad\qquad \forall d, t \in \mathcal{D}, \mathcal{T} \qquad (7i)$$

$$\underline{E}_d \leq \sum_{t \in \mathcal{T}} \left[p_{d,t} \Delta t - r^{\uparrow}_{d,t} \right] \; ; \qquad\qquad \forall d \in \mathcal{D} \qquad (7j)$$

$$\underline{Q}_d \leq \sum_{t \in \mathcal{T}} h_{d,t} \Delta t \; ; \qquad\qquad \forall d \in \mathcal{D} \qquad (7k)$$

3.1.6. Remarks

The optimization problem presented in (1)-(7) is a deterministic model for RVPP participation in the electrical energy and reserve markets, as well as for establishing a thermal HPA contract. In the next section, the proposed formulation is developed to incorporate various uncertainties into the optimization problem.

3.2. Robust Formulation

The deterministic formulation presented in Section 3.1 neglects the variation of uncertain parameters. However, uncertainty in electricity energy and reserve market prices can negatively (or positively) affect the RVPP profit. Additionally, uncertainties in the production and demand of RVPP units can lead to reduced production or increased demand, thus impacting RVPP market profits. Therefore, the RVPP operator must account for the effect of various uncertainties in its decision-making process. In the following section, the optimization problem of the RVPP is extended to incorporate these variations.

3.2.1. Two-Stage Robust Model

A two-stage RO problem is formulated in (8) as a max-min problem to account for various uncertain parameters in the objective function and constraints of the optimization problem. In the first stage, the RVPP operator maximizes its objective function (8a), which is analogous to (1). The set of first-stage decision variables, $\Xi^{DA+SR+HPA}$, is also similar to those in the deterministic model. In the second stage, uncertainty adversely impacts the electricity energy and reserve prices in the objective function (8a). This is modeled through the minimization in the inner problem, which is defined for the objective function's uncertainty set $\Xi^O = \{\lambda_t^{DA}, \lambda_t^{SR,\downarrow}, \lambda_t^{SR,\uparrow}\}$. Additionally, uncertainty is modeled to potentially decrease the thermal production of the SF of CSPs and the electrical production of ND-RESs, while increasing the consumption of EDs/TDs, as reflected in constraints (8b)-(8e). The decision variables associated with uncertainty in these constraints are defined by the set $\Xi^C = \{P_{\theta,t}^{SF}, P_{r,t}, P_{d,t}, H_{d,t}\}$. It is important to note that, unlike the deterministic problem, the new sets Ξ^O and Ξ^C include second-stage decision variables, which were parameters in the deterministic problem. The constraints of the deterministic problem described in Section 3.1 that are unaffected by uncertainty are defined in (8f).

$$
\max_{\Xi^{DA+SR+HPA}} \left\{ \min_{\Xi^O} \left\{ \sum_{t \in \mathcal{T}} \left[\lambda_t^{DA} p_t^{DA} \Delta t + \lambda_t^{SR,\uparrow} r_t^{SR,\uparrow} + \lambda_t^{SR,\downarrow} r_t^{SR,\downarrow} \right] \right. \right.
$$
$$
\left. \left. - \sum_{t \in \mathcal{T}} \lambda_t^{HT} h_t^{HT} \Delta t - \sum_{t \in \mathcal{T}} \sum_{r \in \mathcal{R}} C_r p_{r,t} \Delta t - \sum_{t \in \mathcal{T}} \sum_{\theta \in \Theta} C_\theta (p_{\theta,t} + h_{\theta,t}) \Delta t \right\} \right\} \tag{8a}
$$

st.

$$
p_{\theta,t}^{SF} \leq \min_{P_{\theta,t}^{SF}} \left\{ P_{\theta,t}^{SF} \right\} ; \qquad\qquad \forall \theta, t \in \Theta, \mathcal{T} \tag{8b}
$$

$$
p_{r,t} + r_{r,t}^{\uparrow} \leq \min_{P_{r,t}} \{ P_{r,t} \} ; \qquad\qquad \forall r, t \in \mathcal{R}, \mathcal{T} \tag{8c}
$$

$$
p_{d,t} \geq - \min_{P_{d,t}} \{ -P_{d,t} \} ; \qquad\qquad \forall d, t \in \mathcal{D}, \mathcal{T} \tag{8d}
$$

$$
h_{d,t} \geq - \min_{H_{d,t}} \{ -H_{d,t} \} ; \qquad\qquad \forall d, t \in \mathcal{D}, \mathcal{T} \tag{8e}
$$

$$
(2), (3b) - (3d), (3f) - (3h), (4), (5), (6b) - (6d), (7c) - (7k) ; \tag{8f}
$$

In this section, a flexible risk-averse strategy is developed by extending the theory of RO presented in [43] and the forward-backward asymmetric RO approach in [47] to model the behavior of the RVPP operator under uncertain parameters. Flexibility in addressing uncertainty is achieved through the use of the *uncertainty budget* parameter, which is applied to both the objective function (i.e., Γ^{DA}, $\Gamma^{SR,\uparrow}$, and $\Gamma^{SR,\downarrow}$) and the constraints (Γ_θ, Γ_r, and Γ_d) of the optimization problem. Each uncertainty budget is defined as an integer value ranging from 0 to 24 over the full scheduling horizon (i.e., 24 hours), and it determines the level of conservatism adopted by the RVPP operator. Mathematically, the uncertainty budget specifies the number of time periods during which uncertain parameters (such as market prices or ND-RES generation) are allowed to deviate from their nominal (forecasted) values. A lower uncertainty budget leads to a more optimistic (less robust) solution, while a higher budget increases conservatism by accounting for more potential deviations. For instance, electricity market price uncertainties are modeled using asymmetric uncertainty bounds, defined as $\lambda_t^{DA} \in \left[\tilde{\lambda}_t^{DA} - \check{\lambda}_t^{DA}, \tilde{\lambda}_t^{DA} + \hat{\lambda}_t^{DA} \right]$, where in general, $\check{\lambda}_t^{DA} \neq \hat{\lambda}_t^{DA}$. In the defined bound, the worst-case electricity prices are determined based on the direction of the RVPP's traded energy in a given period; i.e., the minimum price represents the worst case when the RVPP is selling energy, and the

19

maximum price represents the worst case when the RVPP is buying energy. For the uncertainty of up/down reserve prices $\left(\lambda_t^{SR,\uparrow}\in\left[\hat{\tilde{\lambda}}_t^{SR,\uparrow}-\check{\lambda}_t^{SR,\uparrow},\hat{\tilde{\lambda}}_t^{SR,\uparrow}\right]\right.$ and $\left.\lambda_t^{SR,\downarrow}\in\left[\hat{\tilde{\lambda}}_t^{SR,\downarrow}-\check{\lambda}_t^{SR,\downarrow},\hat{\tilde{\lambda}}_t^{SR,\downarrow}\right]\right)$, thermal production of SF of CSPs $\left(P_{\theta,t}^{SF}\in\left[\hat{\tilde{P}}_{\theta,t}^{SF}-\check{P}_{\theta,t}^{SF},\hat{\tilde{P}}_{\theta,t}^{SF}\right]\right)$, and electrical production of ND-RESs $\left(P_{r,t}\in\left[\hat{\tilde{P}}_{r,t}-\check{P}_{r,t},\hat{\tilde{P}}_{r,t}\right]\right)$, only negative deviations are considered, while for EDs/TDs $\left(P_{d,t}\in\left[\check{\tilde{P}}_{d,t},\check{\tilde{P}}_{d,t}+\hat{P}_{d,t}\right]\right.$ and $\left.H_{d,t}\in\left[\check{\tilde{H}}_{d,t},\check{\tilde{H}}_{d,t}+\hat{H}_{d,t}\right]\right)$, only positive deviations are taken into account. This ensures that the worst-case scenario, according to the strategy or level of conservatism chosen by the RVPP operator through the uncertainty budgets, is appropriately represented in the optimization problem, as deviations in opposite directions would result in higher profits for the RVPP.

The objective function (9a) is formulated by considering the defined bounds for different uncertain parameters in the objective function of the problem. The inner maximization problem in (9a) identifies the worst-case scenario for RVPP profit across different market participation. This is achieved by introducing new time period sets $\mathcal{T}^{DA}$, $\mathcal{T}^{SR,\uparrow}$, and $\mathcal{T}^{SR,\downarrow}$, which represent the periods where price deviations from the median value or higher bound have the greatest negative impact on the RVPP's profit. Since the cost of purchased thermal energy through HPA, the operation costs of ND-RES and CSPs, as well as the RVPP's profit for median values of DAM price and upper bound of SRM price of uncertain parameters, are not influenced by these uncertainties, the corresponding terms can be moved to the outer-layer problem. Additionally, a new positive auxiliary variable y_t^{DA} is introduced to represent the traded electrical energy in (9a). This variable is bounded by constraint (9b), effectively modeling the asymmetric behavior of electricity price uncertainties based on the direction of traded energy in the market.

Equations (9c)-(9f) address the uncertainty in the thermal production of SF of CSPs, electrical production of ND-RESs, and EDs/TDs consumption, respectively. These constraints are developed by incorporating the described uncertainty bounds and the newly defined worst-case sets $\mathcal{T}_\theta$, $\mathcal{T}_r$, and $\mathcal{T}_d$ for each time period. For example, in constraint (9c), the worst-case deviation of thermal power due to uncertainty, $\check{P}_{\theta,t'}^{SF}$, is reduced from the upper bound of forecast value $\hat{\tilde{P}}_{\theta,t}^{SF}$ only when t' corresponds to period t and belongs to the set $\mathcal{T}_\theta$ (i.e., $t'\in\mathcal{T}_\theta, t'=t$). Physically, $\hat{\tilde{P}}_{\theta,t}^{SF}$ represents the nominal upper bound of thermal power expected under ideal solar conditions, while $\check{P}_{\theta,t'}^{SF}$ captures the maximum possible reduction from this value due to adverse effects such as cloud cover or irradiance variability. This constraint ensures that the available thermal power of the SF is robustly limited by accounting for possible underproduction within a predefined uncertainty budget Γ_θ. The formulation effectively captures a flexible adversarial scenario in which the actual thermal power output from the SF is reduced to account for forecast errors and unforeseen fluctuations in solar irradiation. This uncertain constraint has a direct impact on the downstream operation of the TS and PB systems, as outlined by constraints (3)-(5) in Section 3.1.3. Specifically, a reduction in $p_{\theta,t}^{SF}$ due to solar forecast uncertainty can limit the thermal input to TS and PB, thereby constraining the electrical energy and reserve that the CSP can commit. The positive nature of the auxiliary variables is established in (9g), while constraint (9h) is identical to (8f).

$$\max_{\Xi^{DA+SR+HPA}}\left\{-\sum_{t\in\mathcal{T}}\lambda_t^{HT}h_t^{HT}\Delta t-\sum_{t\in\mathcal{T}}\sum_{r\in\mathcal{R}}C_r p_{r,t}\Delta t-\sum_{t\in\mathcal{T}}\sum_{\theta\in\Theta}C_\theta(p_{\theta,t}+h_{\theta,t})\Delta t\right.$$
$$\left.+\sum_{t\in\mathcal{T}}\left[\tilde{\lambda}_t^{DA}p_t^{DA}\Delta t+\hat{\tilde{\lambda}}_t^{SR,\uparrow}r_t^{SR,\uparrow}+\hat{\tilde{\lambda}}_t^{SR,\downarrow}r_t^{SR,\downarrow}\right]\right.$$

$$- \max_{\left\{ \substack{\mathcal{T}^{DA}, \\ \mathcal{T}^{SR,\uparrow}, \\ \mathcal{T}^{SR,\downarrow}} \middle| \substack{|\mathcal{T}^{DA}|=\Gamma^{DA}, \\ |\mathcal{T}^{SR,\uparrow}|=\Gamma^{SR,\uparrow}, \\ |\mathcal{T}^{SR,\downarrow}|=\Gamma^{SR,\downarrow}} \right\}} \left\{ \sum_{t \in \mathcal{T}^{DA}} \check{\lambda}_t^{DA} y_t^{DA} + \sum_{t \in \mathcal{T}^{SR,\uparrow}} \check{\lambda}_t^{SR,\uparrow} r_t^{SR,\uparrow} + \sum_{t \in \mathcal{T}^{SR,\downarrow}} \check{\lambda}_t^{SR,\downarrow} r_t^{SR,\downarrow} \right\} \right\} \quad (9a)$$

st.

$$- \frac{\check{\lambda}_t^{DA}}{\hat{\lambda}_t^{DA}} y_t^{DA} \leq p_t^{DA} \Delta t \leq y_t^{DA} ; \qquad \forall t \in \mathcal{T} \quad (9b)$$

$$p_{\theta,t}^{SF} \leq \hat{\check{P}}_{\theta,t}^{SF} - \max_{\{\mathcal{T}_\theta | \ |\mathcal{T}_\theta|=\Gamma_\theta\}} \left\{ \sum_{t' \in \mathcal{T}_\theta, t'=t} \check{P}_{\theta,t'}^{SF} \right\} ; \qquad \forall \theta, t \in \Theta, \mathcal{T} \quad (9c)$$

$$p_{r,t} + r_{r,t}^{\uparrow} \leq \hat{\check{P}}_{r,t} - \max_{\{\mathcal{T}_r | \ |\mathcal{T}_r|=\Gamma_r\}} \left\{ \sum_{t' \in \mathcal{T}_r, t'=t} \check{P}_{r,t'} \right\} ; \qquad \forall r, t \in \mathcal{R}, \mathcal{T} \quad (9d)$$

$$p_{d,t} \geq \check{\check{P}}_{d,t} + \max_{\{\mathcal{T}_d | \ |\mathcal{T}_d|=\Gamma_d\}} \left\{ \sum_{t' \in \mathcal{T}_d, t'=t} \hat{P}_{d,t'} \right\} ; \qquad \forall d, t \in \mathcal{D}, \mathcal{T} \quad (9e)$$

$$h_{d,t} \geq \check{\tilde{H}}_{d,t} + \max_{\{\mathcal{T}_d | \ |\mathcal{T}_d|=\Gamma_d\}} \left\{ \sum_{t' \in \mathcal{T}_d, t'=t} \hat{H}_{d,t'} \right\} ; \qquad \forall d, t \in \mathcal{D}, \mathcal{T} \quad (9f)$$

$$y_t^{DA} \geq 0 ; \qquad \forall t \in \mathcal{T} \quad (9g)$$

$$(2), (3b) - (3d), (3f) - (3h), (4), (5), (6b) - (6d), (7c) - (7k) ; \quad (9h)$$

3.2.2. Inner Problems Reformulation

Although the maximization term in the last part of the objective function (9a) (the protection function) captures the worst-case scenario for the uncertain parameters, the process of selecting values based on the defined sets can be expressed in a linear manner. To achieve this, assuming the optimal values (indicated with superscript *) of the upper-level variables $y_t^{DA^*}$, $r_t^{SR,\uparrow^*}$, and $r_t^{SR,\downarrow^*}$ and using Proposition 1 from [43], linear problem (10) is equivalent to the protection function in (9a). Constraints (10b)-(10d) limit the summation of the new auxiliary variables z_t^{DA}, $z_t^{SR,\uparrow}$, and $z_t^{SR,\downarrow}$ for each uncertain parameter in the objective function of the problem to the corresponding uncertainty budgets Γ^{DA}, $\Gamma^{SR,\uparrow}$, and $\Gamma^{SR,\downarrow}$, respectively. These constraints ensure that the positive auxiliary variables z_t^{DA}, $z_t^{SR,\uparrow}$, and $z_t^{SR,\downarrow}$ are less or equal than 1, thereby achieving the same optimal value for the objective function in (10a) and the protection function in (9a). The dual variables of each constraint are defined in these equations, which are then used in Section 3.2.3 to derive the final MILP formulation.

$$\max \left\{ \sum_{t \in \mathcal{T}^{DA}} \check{\lambda}_t^{DA} y_t^{DA^*} z_t^{DA} + \sum_{t \in \mathcal{T}^{SR,\uparrow}} \check{\lambda}_t^{SR,\uparrow} r_t^{SR,\uparrow^*} z_t^{SR,\uparrow} + \sum_{t \in \mathcal{T}^{SR,\downarrow}} \check{\lambda}_t^{SR,\downarrow} r_t^{SR,\downarrow^*} z_t^{SR,\downarrow} \right\} \quad (10a)$$

st.

$$\sum_{t \in \mathcal{T}^{DA}} z_t^{DA} \leq \Gamma^{DA} : \phi^{DA} ; \quad (10b)$$

$$\sum_{t \in \mathcal{T}^{SR,\uparrow}} z_t^{SR,\uparrow} \leq \Gamma^{SR,\uparrow} : \phi^{SR,\uparrow} ; \quad (10c)$$

$$\sum_{t \in \mathcal{T}^{SR,\downarrow}} z_t^{SR,\downarrow} \leq \Gamma^{SR,\downarrow} : \phi^{SR,\downarrow} ; \tag{10d}$$

$$0 \leq z_t^{DA} \leq 1 : \zeta_t^{DA} ; \qquad\qquad \forall t \in \mathcal{T}^{DA} \tag{10e}$$

$$0 \leq z_t^{SR,\uparrow} \leq 1 : \zeta_t^{SR,\uparrow} ; \qquad\qquad \forall t \in \mathcal{T}^{SR,\uparrow} \tag{10f}$$

$$0 \leq z_t^{SR,\downarrow} \leq 1 : \zeta_t^{SR,\downarrow} ; \qquad\qquad \forall t \in \mathcal{T}^{SR,\downarrow} \tag{10g}$$

The equivalent linear formulation for selecting the worst-case scenarios of thermal production uncertainty of SF of CSP in constraint (9c) is presented as linear formulation (11). The objective function (11a) maximizes the thermal production deviation caused by uncertainty in the corresponding period t ($t' \in \mathcal{T}_\theta$, $t' = t$). The summation of the auxiliary positive variables $z_{\theta,t'}$ for the corresponding period t and other worst-case periods, which are fixed at their optimal values, is constrained to be less than the uncertainty budget Γ_θ. The bound for the auxiliary variable $z_{\theta,t'}$ is defined in (11c). Worth noting that the linear formulation (11) considers the temporal constraints of the uncertainty parameter over the entire operation period, rather than defining the worst case of the uncertain parameter in a single period, as done in [1, 35, 37]. This feature allows the RVPP to adjust a single uncertain parameter for the entire period instead of multiple parameters for each time period and uncertain parameter.

The equivalent linear formulations for worst-case selection in constraints (9d)-(9f), addressing ND-RES production, and EDs/TDs uncertainty, respectively, can be derived similarly to (11). These are omitted here for brevity.

$$\max \sum_{t' \in \mathcal{T}_\theta, t'=t} \check{P}_{\theta,t'}^{SF} z_{\theta,t'} ; \qquad\qquad \forall \theta, t \in \Theta, \mathcal{T} \tag{11a}$$

st.

$$\sum_{t' \in \mathcal{T}_\theta, t'=t} z_{\theta,t'} + \sum_{t' \in \mathcal{T}_\theta, t' \neq t} z_{\theta,t'}^* \leq \Gamma_\theta : \phi_\theta ; \tag{11b}$$

$$0 \leq z_{\theta,t'} \leq 1 : \zeta_{\theta,t'} ; \qquad\qquad \forall t' \in \mathcal{T}_\theta, t' = t \tag{11c}$$

3.2.3. MILP Formulation

By applying strong duality [48] to the linear formulations in (10) and (11) (and similarly for equivalent linear formulations related to other uncertain constraints), and replacing their dual problems instead of the protection function in the objective function (9a) and the protection functions in the constraints (9c)-(9f), respectively, the final MILP is formulated as (12). The first and second lines of the objective function (12a) are identical to the first and second lines of (9a). The third line captures the negative effects of uncertainties in electricity (energy and reserve) prices. Constraint (12b) is equivalent to (9b). Constraints (12c)-(12e) are the dual constraints of the linear problem related to electricity prices uncertainties in (10). Constraint (12f) represents the upper limit of thermal production of SF of CSP while accounting for uncertainty. Since the term $\Gamma_\theta - \sum_{t' \in \mathcal{T}_\theta, t' \neq t} z_{\theta,t'}^*$ in (11b) can only take a value of zero or one, depending on the number of worst-case periods in its defined set, a new binary variable $\chi_{\theta,t}$ is introduced to represent these conditions. Additionally, a new positive auxiliary variable $y_{\theta,t}$ is defined in (12f) and constrained in (12g) using the big-M method [48] to represent the dual term $\chi_{\theta,t}\phi_\theta + \zeta_{\theta,t}$. Constraint (12h) is the dual constraint of the linear problem associated with CSP thermal production uncertainty in (11). Constraint (12i) assigns the uncertainty budget for thermal

22

production of SF of CSP. Constraints (12j)-(12m) represent the ND-RESs electrical production uncertain constraints, constraints (12n)-(12s) represent the EDs/TDs uncertain constraints. These constraints are defined similarly to the thermal production uncertainty of SF of CSP constraints (12f)-(12i). The main difference is that, for EDs/TDs, the worst-case uncertainty results in an increase in these parameters, whereas, for thermal production of SF of CSP and ND-RES electrical production, it results in a decrease. The deterministic constraints that remain unaffected by uncertainty are outlined in (12t). Finally, the nature of the positive and binary variables is defined in (12u)-(12w).

It is worth noting that the refined MILP formulation in (12) is developed to flexibly consider both source- and load-side uncertainty by adjusting the uncertainty budget defined for temporal constraints. The flexibility to address different levels of uncertainty and the computational efficiency of the proposed approach are extensively studied through various case studies in Section 4.

$$
\max_{\Xi^{DA+SR+HPA}} \Bigg\{ -\sum_{t\in\mathcal{T}} \lambda_t^{HT} h_t^{HT} \Delta t - \sum_{t\in\mathcal{T}}\sum_{r\in\mathcal{R}} C_r p_{r,t} \Delta t - \sum_{t\in\mathcal{T}}\sum_{\theta\in\Theta} C_\theta (p_{\theta,t} + h_{\theta,t}) \Delta t
$$
$$
+ \sum_{t\in\mathcal{T}} \left[\tilde{\lambda}_t^{DA} p_t^{DA} \Delta t + \hat{\tilde{\lambda}}_t^{SR,\uparrow} r_t^{SR,\uparrow} + \hat{\tilde{\lambda}}_t^{SR,\downarrow} r_t^{SR,\downarrow} \right]
$$
$$
- \Gamma^{DA} \phi^{DA} - \Gamma^{SR,\uparrow} \phi^{SR,\uparrow} - \Gamma^{SR,\downarrow} \phi^{SR,\downarrow} - \sum_{t\in\mathcal{T}} \left[\zeta_t^{DA} + \zeta_t^{SR,\uparrow} + \zeta_t^{SR,\downarrow} \right] \Bigg\} \tag{12a}
$$

st.

$$
-\frac{\check{\lambda}_t^{DA}}{\hat{\lambda}_t^{DA}} y_t^{DA} \le p_t^{DA} \Delta t \le y_t^{DA} ; \qquad\qquad \forall t \in \mathcal{T} \tag{12b}
$$

$$
\phi^{DA} + \zeta_t^{DA} \ge \check{\lambda}_t^{DA} y_t^{DA} ; \qquad\qquad \forall t \in \mathcal{T} \tag{12c}
$$

$$
\phi^{SR,\uparrow} + \zeta_t^{SR,\uparrow} \ge \check{\lambda}_t^{SR,\uparrow} r_t^{SR,\uparrow} ; \qquad\qquad \forall t \in \mathcal{T} \tag{12d}
$$

$$
\phi^{SR,\downarrow} + \zeta_t^{SR,\downarrow} \ge \check{\lambda}_t^{SR,\downarrow} r_t^{SR,\downarrow} ; \qquad\qquad \forall t \in \mathcal{T} \tag{12e}
$$

$$
p_{\theta,t}^{SF} \le \hat{\tilde{P}}_{\theta,t}^{SF} - \chi_{\theta,t} \phi_\theta - \zeta_{\theta,t} = \hat{\tilde{P}}_{\theta,t}^{SF} - y_{\theta,t} ; \qquad\qquad \forall \theta,t \in \Theta,\mathcal{T} \tag{12f}
$$

$$
\phi_\theta + \zeta_{\theta,t} - M(1 - \chi_{\theta,t}) \le y_{\theta,t} \le M\chi_{\theta,t} ; \qquad\qquad \forall \theta,t \in \Theta,\mathcal{T} \tag{12g}
$$

$$
\phi_\theta + \zeta_{\theta,t} \ge \check{P}_{\theta,t} ; \qquad\qquad \forall \theta,t \in \Theta,\mathcal{T} \tag{12h}
$$

$$
\sum_t \chi_{\theta,t} = \Gamma_\theta ; \qquad\qquad \forall \theta \in \Theta \tag{12i}
$$

$$
p_{r,t} + r_{r,t}^\uparrow \le \hat{\tilde{P}}_{r,t} - \chi_{r,t} \phi_r - \zeta_{r,t} = \hat{\tilde{P}}_{r,t} - y_{r,t} ; \qquad\qquad \forall r,t \in \mathcal{R},\mathcal{T} \tag{12j}
$$

$$
\phi_r + \zeta_{r,t} - M(1 - \chi_{r,t}) \le y_{r,t} \le M\chi_{r,t} ; \qquad\qquad \forall r,t \in \mathcal{R},\mathcal{T} \tag{12k}
$$

$$
\phi_r + \zeta_{r,t} \ge \check{P}_{r,t} ; \qquad\qquad \forall r,t \in \mathcal{R},\mathcal{T} \tag{12l}
$$

$$
\sum_t \chi_{r,t} = \Gamma_r ; \qquad\qquad \forall r \in \mathcal{R} \tag{12m}
$$

$$
p_{d,t} \ge \check{\tilde{P}}_{d,t} + \chi_{d,t} \phi_d + \zeta_{d,t} = \check{\tilde{P}}_{d,t} + y_{d,t} ; \qquad\qquad \forall d,t \in \mathcal{D},\mathcal{T} \tag{12n}
$$

$$
h_{d,t} \ge \check{\tilde{H}}_{d,t} + \chi_{d,t} \phi_d + \zeta_{d,t} = \check{\tilde{H}}_{d,t} + y_{d,t} ; \qquad\qquad \forall d,t \in \mathcal{D},\mathcal{T} \tag{12o}
$$

$$
\phi_d + \zeta_{d,t} - M(1 - \chi_{d,t}) \le y_{d,t} \le M\chi_{d,t} ; \qquad\qquad \forall d,t \in \mathcal{D},\mathcal{T} \tag{12p}
$$

$$
\phi_d + \zeta_{d,t} \ge \hat{P}_{d,t} ; \qquad\qquad \forall d,t \in \mathcal{D},\mathcal{T} \tag{12q}
$$

23

$$\phi_d + \zeta_{d,t} \geq \hat{H}_{d,t} \; ; \qquad\qquad \forall d, t \in \mathcal{D}, \mathcal{T} \qquad (12\text{r})$$

$$\sum_t \chi_{d,t} = \Gamma_d \; ; \qquad\qquad \forall d \in \mathcal{D} \qquad (12\text{s})$$

$$(2), (3\text{b}) - (3\text{d}), (3\text{f}) - (3\text{h}), (4), (5), (6\text{b}) - (6\text{d}), (7\text{c}) - (7\text{k}) \; ; \qquad (12\text{t})$$

$$\phi^{DA}, \phi^{SR,\uparrow}, \phi^{SR,\downarrow}, \zeta_t^{DA}, \zeta_t^{SR,\uparrow}, \zeta_t^{SR,\downarrow}, y_t^{DA} \geq 0 \; ; \qquad\qquad \forall t \in \mathcal{T} \qquad (12\text{u})$$

$$\phi_\theta, \phi_r, \phi_d, \zeta_{\theta,t}, \zeta_{r,t}, \zeta_{d,t}, y_{\theta,t}, y_{r,t}, y_{d,t} \geq 0 \; ; \qquad \forall \theta, r, d, t \in \Theta, \mathcal{R}, \mathcal{D}, \mathcal{T} \qquad (12\text{v})$$

$$\chi_{\theta,t}, \chi_{r,t}, \chi_{d,t} \in \{0, 1\} \; ; \qquad \forall \theta, r, d, t \in \Theta, \mathcal{R}, \mathcal{D}, \mathcal{T} \qquad (12\text{w})$$

3.2.4. Flexibility Metrics

In this paper, the flexibility of each RVPP unit is quantified as the total upward or downward reserve it provides over the scheduling horizon. Additionally, normalized definitions are employed, where the upward or downward reserve is expressed as a ratio relative to the capacity of each RVPP unit.

Specifically, the flexibility is quantified using the metrics of total upward reserve, as presented in equation (13a), and total downward reserve, as calculated in equation (13b), where $r_{u,t}^{\uparrow}$ and $r_{u,t}^{\downarrow}$ represent the upward and downward reserve provided by unit u at time t. The index $u \in \mathcal{U}$ represents the type of RVPP unit (CSP, ED, and ND-RES).

$$\sum_{t \in \mathcal{T}} r_{u,t}^{\uparrow} \; ; \qquad\qquad \forall u \in \mathcal{U} \qquad (13\text{a})$$

$$\sum_{t \in \mathcal{T}} r_{u,t}^{\downarrow} \; ; \qquad\qquad \forall u \in \mathcal{U} \qquad (13\text{b})$$

Additionally, to normalize flexibility contributions by unit capacity and enable fair comparisons across heterogeneous RVPP components, we define the reserve-to-capacity ratio for upward reserve and downward reserve according to equations (14a) and (14b). Where P_u denotes the installed capacity of unit u.

$$\frac{\sum_{t \in \mathcal{T}} r_{u,t}^{\uparrow}}{P_u} \; ; \qquad\qquad \forall u \in \mathcal{U} \qquad (14\text{a})$$

$$\frac{\sum_{t \in \mathcal{T}} r_{u,t}^{\downarrow}}{P_u} \; ; \qquad\qquad \forall u \in \mathcal{U} \qquad (14\text{b})$$

3.2.5. Uncertainty Characterization

The confidence bounds of uncertain parameters can be determined through various methods. These include leveraging historical records with observational and measurement data [49], fitting parametric distributions to model uncertainties [50], and employing bootstrapping techniques for resampling-based estimation [51]. Historical data is derived from past observations and measurements, which can be examined to identify underlying patterns and relationships. Figure 3 illustrates the method used in this paper to assign bounds to uncertain parameters based on historical data. For this purpose, data for various uncertain parameters is collected over a 30-day period. The median, lower bound, and upper bound of these parameters are determined for each hour of the day. To prevent overly conservative solutions, the 20% and 80% percentiles of the data are used as the lower and upper bounds, respectively.
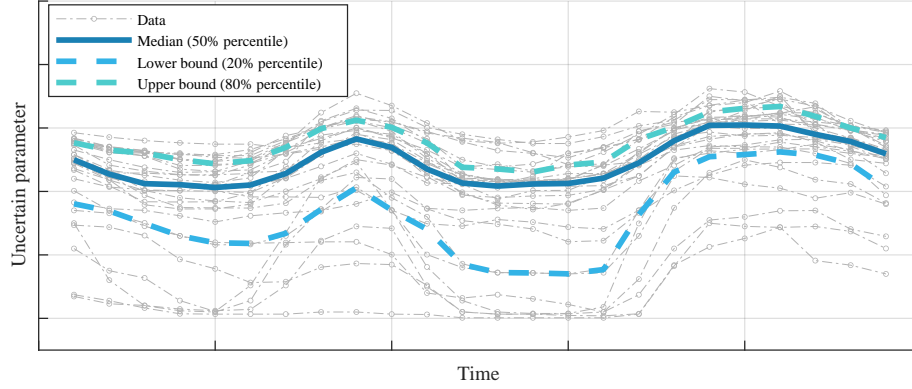
Figure 3: Assigning the bounds of uncertain parameters using historical data.

4. Case Studies

This section presents the simulation results of the proposed two-stage RO model. The simulations are conducted on an RVPP that includes one CSP, two WFs, three solar PV plants, three types of EDs (residential, industrial, and service), and two types of TDs (residential and industrial). The forecast bounds for electrical and thermal energy generation units within the RVPP are illustrated in Figure 4. These bounds are derived using the methodology described in Section 3.2.5, based on historical data from CIEMAT Spain [52] for solar PVs and the CSP, and from Iberdrola Spain [53] for WFs. The economic data, including the ranges of electricity and thermal energy prices, the operational costs of RVPP units, and the forecast bounds for various uncertain parameters, are presented in Table 2. The electrical and thermal energy consumption of the demands is illustrated in Figures 5 and 6, based on the hourly demand profiles provided in [46, 54]. The main technical data related to the demands are provided in Table 3. The technical and design characteristics of the CSP are presented in Tables 4 and 5, based on data from CIEMAT Spain [52] and [4]. The hourly thermal energy output profiles used in this study are adopted from [4], which simulated CSP performance using TMY3-format meteorological data representative of high-Direct Normal Irradiance (DNI) locations in Southern Europe and North Africa. These scenarios, produced for March 2018, inherently account for solar irradiance and other weather variables and are used here as inputs for simulation analysis. The technical information for the ND-RES, including WFs and solar PV plants, is provided in Table 6. The efficiency of thermal-to-electrical energy conversion in the turbine varies depending on the thermal power of the PB, following the piecewise linear relationship depicted in Figure 7. The forecast bounds for DAM and SRM electricity prices, derived from historical data in [55], are shown in Figure 8. The cost of purchasing thermal energy via a HPA is determined by a time-of-use contract between the RVPP and the thermal energy service provider. Figure 8 illustrates the HPA price at different hours of the day, estimated based on the costs associated with thermal energy production using various technologies in Spain [56]. Table 7 provides information on the assumed uncertainty budget for different uncertain parameters across various case studies. Since the production of solar PVs and the SF of CSP is zero during night hours, a lower uncertainty budget is considered for these units. In this way, the percentage of hours with deviations over the 24-hour period is defined within the same range for all uncertain parameters.

Three case studies are performed to assess the effectiveness of the proposed model. In the first case study, the scheduling of RVPP units and the traded electrical and thermal energy of RVPP are obtained without considering uncertainty. The thermal-to-electrical energy conversion of CSP, the energy in its different

25

elements, and the proposed approach to adjusting a share of TS energy for reserve provision are studied. In the second case study, the performance of the proposed two-stage RO approach in handling different uncertainties—such as electricity price, ND-RES production, thermal production of CSP, and consumption
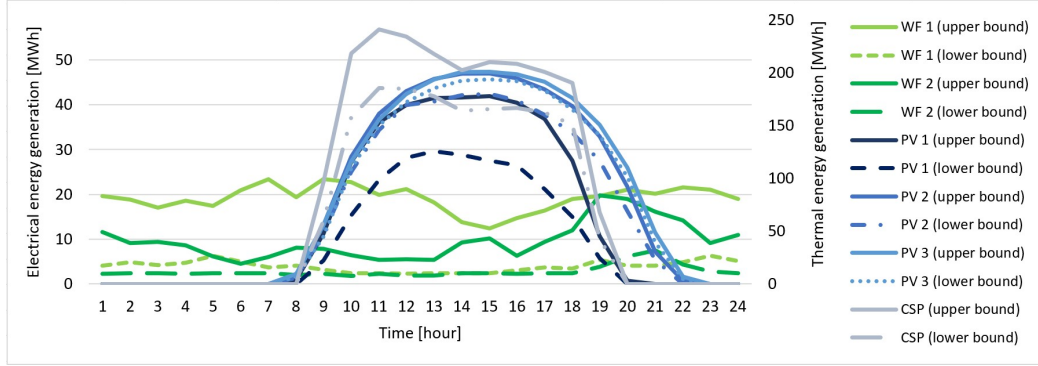

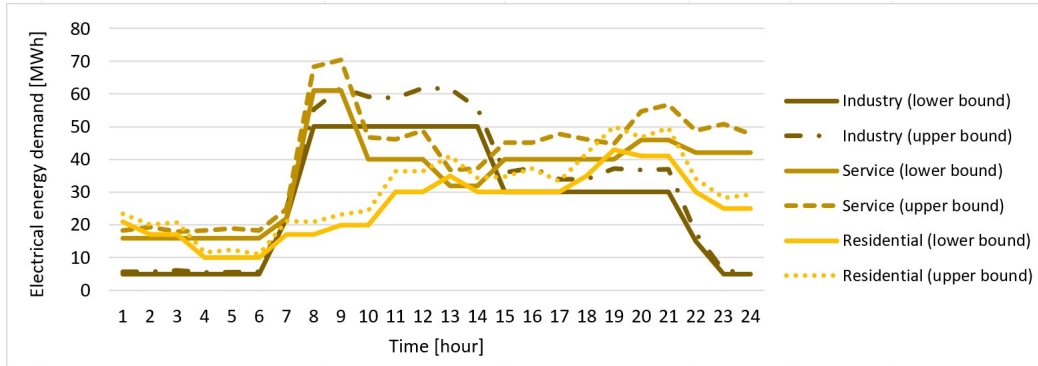Figure 4: The forecast bounds of WFs, solar PVs, and CSP.

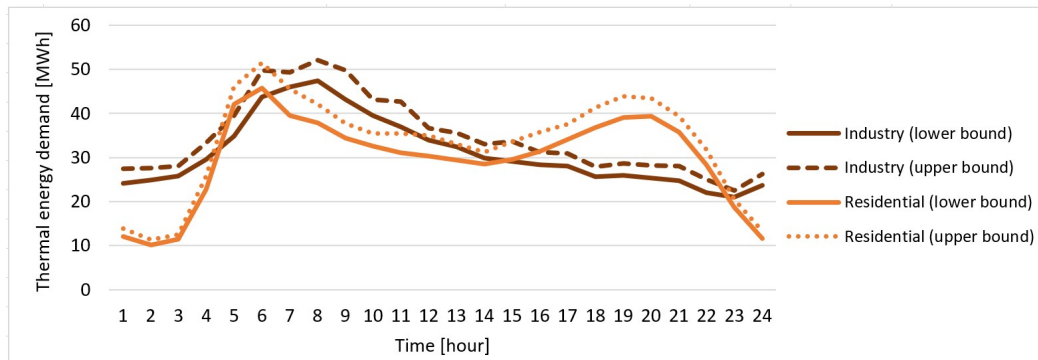Figure 5: The forecast bounds of EDs.
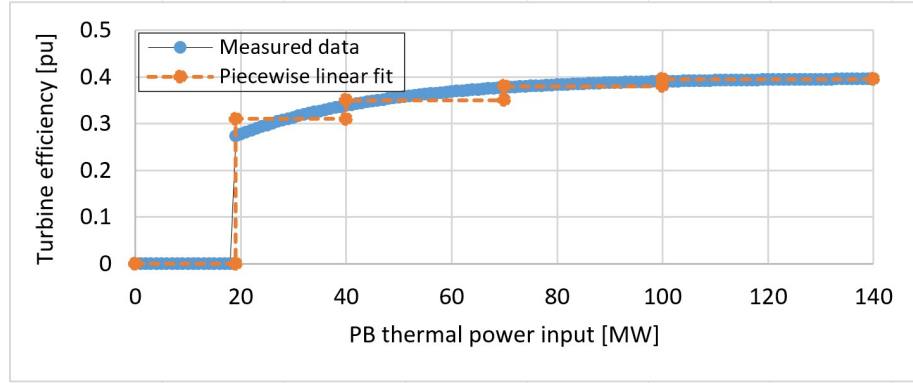

Figure 6: The forecast bounds of TDs.

Figure 7: Thermal to electrical conversion efficiency of PB.
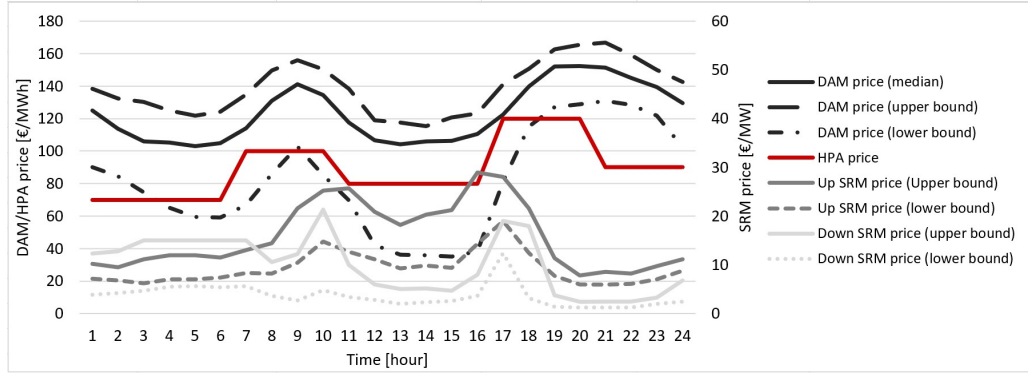
Figure 8: The DAM, SRM, and HPA price data.

Table 2: Economic data.

Market data	Value
DAM price ranges [€/MWh]	35-167
Up SRM price ranges [€/MW]	6-29
Down SRM price ranges [€/MW]	1-22
HPA price ranges [€/MW]	70-120

Operation cost data	Value
CSP operation cost [€/MWh]	25
WF operation cost [€/MWh]	15
PV operation cost [€/MWh]	7.5

Uncertain data	Value
Forecast percentile [%]	20-80

Table 3: ED and TD data.

Parameter	ED			TD	
	Industry	**Service**	**Residential**	**Industry**	**Residential**
Minimum energy consumption [MWh]	600	800	600	700	700
Minimum power output [MW]	2	10	5	10	5
Maximum power output [MW]	70	80	60	80	70
Initial power output [MW]	5	42	25	23	11
Secondary reserve ramp rate [MW/min]	30	25	10	-	-
Secondary reserve relative to the power capacity [%]	10	10	10	-	-

Table 4: CSP data.

SF	
SF maximum thermal power output [MW]	300
PB/Turbine	
PB maximum thermal power input [MW]	140
Turbine maximum electrical power output [MW]	55
Turbine minimum electrical power output [MW]	5
Turbine minimum up/down time [hour]	6
CSP output thermal power efficiency [%]	90
CSP secondary reserve ramp rate [MW/min]	25
CSP secondary reserve relative to power capacity [%]	50
TS	
Maximum thermal energy [MWh]	1100
Minimum thermal energy [MWh]	110
Discharging thermal power [MW]	115
Charging thermal power [MW]	140
Dis/charging efficiency [%]	95

of EDs/TDs—is studied for three different RVPP operator strategies (optimistic, balanced, and pessimistic) against uncertainty. In the third case study, the profitability of RVPP under different market (contract) participation strategies and various decision-making approaches for managing uncertainties is evaluated to demonstrate the effectiveness of the proposed coordinated approach compared to separate market participation strategies. Furthermore, the effect of different possible future prices of HPA (scenarios with thermal energy production from renewable resources rather than fossil fuels) [56] is evaluated. In the fourth case study, the performance of the proposed two-stage RO approach is compared to the SP approach proposed in [2] using out-of-sample assessment.

The characteristics of these three case studies are summarized as follows:

- Case 1: Identify the deterministic optimal operation of RVPP units, including CSP, for supplying both EDs/TDs. Additionally, determine the RVPP's bidding strategy in the electrical energy market and its participation in thermal HPA contract.

28

Table 5: CSP main design data.

SF characteristics	Value
Concentrating solar technology	Parabolic-trough
Heat transfer fluid	Oil
Heat transfer fluid temperature range [°C]	296-390
Receiver type	Tube
Mirror area [m^2]	3270
TS medium	2-tank with molten salt
TS capacity [MWh]	1100
TS duration [h]	7.5
Turbine type or cycle	Rankine steam cycle
PB efficiency [%]	27-40

Table 6: ND-RES data.

Parameter	PV	WF
Maximum/minimum power output [MW]	50/0	50/0
Secondary reserve ramp up rate [MW/min]	10	15
Secondary reserve ramp down rate [MW/min]	25	25
Secondary reserve relative to power capacity [%]	10	10

Table 7: Uncertainty budgets for different uncertain parameters for different RVPP strategies (optimistic, balanced, and pessimistic).

Strategy	DAM/SRM prices	WFs production	PVs production	SF thermal production	EDs/TDs consumption
Optimistic	3	3	2	2	3
Balanced	6	6	4	4	6
Pessimistic	9	9	6	6	9

- Case 2: Assess the optimal bidding strategy of the RVPP while accounting for uncertainties related to DAM and SRM prices, ND-RES production, and variations in EDs/TDs.

- Case 3: Analyze the RVPP's profitability under different market (contract) participation strategies, considering different decision-making approaches to manage uncertainties.

- Case 4: Compare the performance of the proposed two-stage RO approach with the SP model in [2], considering different decision-making approaches in the proposed model and varying numbers of scenarios in [2].

Simulations are conducted on a Dell XPS equipped with an i7-1165G7 2.8 GHz processor and 16 GB of RAM using the CPLEX solver in GAMS 39.1.1. The computation time for all simulations remains under 5 seconds, demonstrating the computational efficiency of the proposed two-stage RO approach for RVPP market participation.

4.1. Case 1

Figure 9 shows the traded electrical energy and reserve of the RVPP in the DAM and SRM, as well as the cumulative energy of the RVPP units for the deterministic case. The figure illustrates that the RVPP is an energy seller in the DAM between hours 10–19, and an energy buyer during other hours. This is due to the high available power from solar PVs and CSP production during hours 10-19. In the night and early morning hours (1–6), the EDs are low and are mainly provided by the WFs. However, the RVPP buys a small amount of energy during these hours to maintain supply and demand balance. Between hours 7–9, the demand increases, and solar PV production is minimal or zero. As a result, the RVPP buys a larger amount of energy during these hours to supply its demands. The CSP turbine starts up at hour 10 and produces electrical energy between hours 10–13 to supply the morning demand and between hours 17–22 to supply the evening demand (when solar PVs production is not at its maximum and demand is high). The RVPP provides upward reserve in the SRM between hours 8–24 and downward reserve in all hours. The upward reserve is mainly provided by the CSP between hours 10–18 and 23–24, and by the demands between hours 8–18. The demands also provide downward reserve throughout all hours. Since the operational cost of the CSP is higher than that of solar PVs and WFs, these units only produce energy and do not provide reserve.

Figure 10 shows the thermal energy traded through the HPA contract, along with the thermal production and demands of the RVPP. The CSP provides all the energy for TDs between hours 7–24. This energy is supplied either by discharging the TS during hours when the sun is not available, by using the SF of the CSP, or by a combination of both. During the night hours (1–6), the thermal energy for demands is provided through the HPA contract. These hours are selected for buying thermal energy since the price of thermal energy is lower compared to other hours (see Figure 8). Additionally, by purchasing thermal energy through the HPA contract during these hours, the CSP can retain enough energy to supply both EDs/TDs during the morning hours.

Figure 11 shows the energy and charging/discharging power of the TS of the CSP. The figure illustrates that the TS discharges during hours 7, 8, 10, and 19–24. In hours 7 and 8, as discussed in Figure 10, the discharged power of the TS is used to supply the local TDs of the RVPP. In hour 10, the discharging power of the TS assists the CSP turbine in starting up and producing electricity. Between hours 19 and 24, the discharged power of the TS is used to support the turbine and/or supply TDs. Figure 11 also shows additional margins compared to the maximum and minimum energy levels of the TS, which are allocated solely for providing reserve. These margins are determined by the optimization problem to avoid the complete
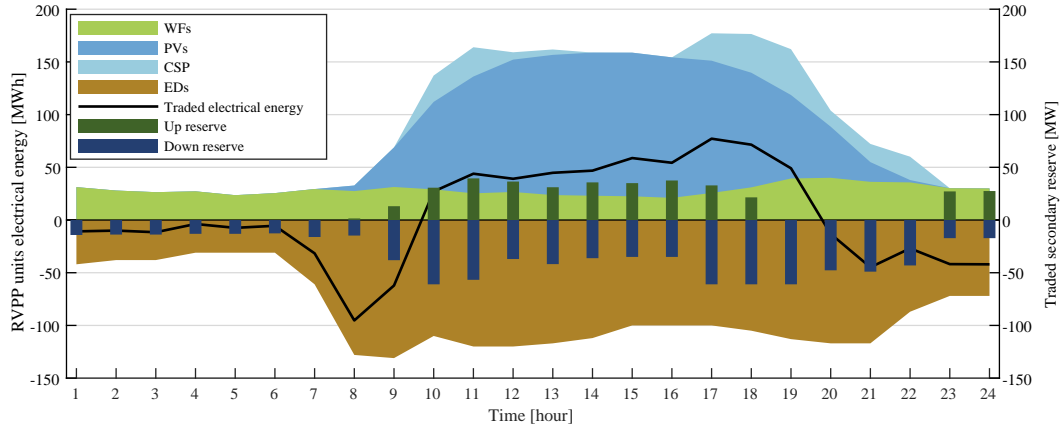

Figure 9: The RVPP traded electrical energy in DAM and traded reserve in SRM, and electrical energy of RVPP units.
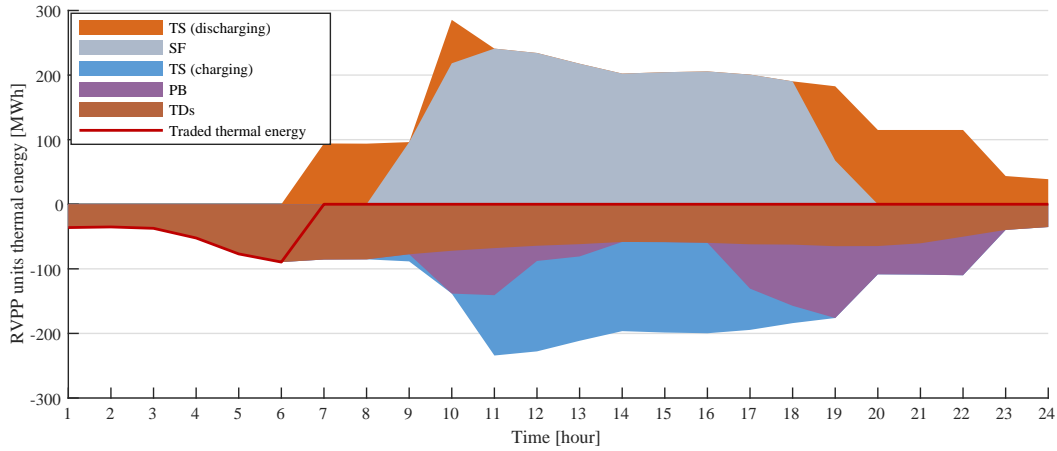
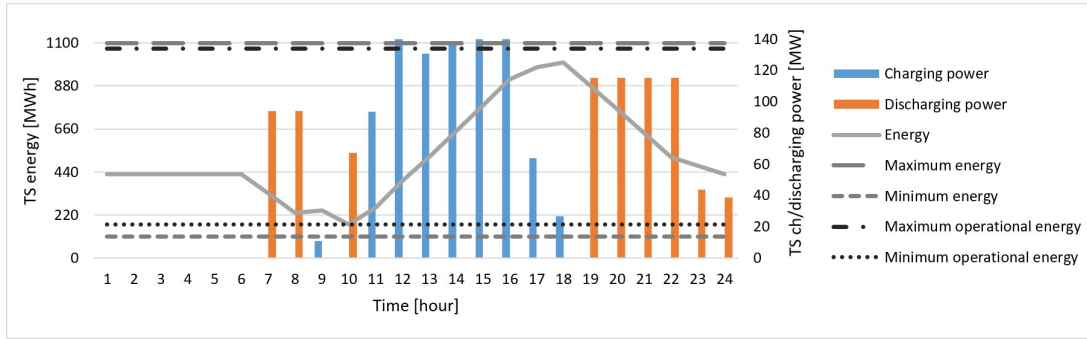Figure 10: The RVPP thermal energy through HPA and thermal energy of RVPP units.

Figure 11: The TS energy and charging/discharging power.

depletion or operation at the maximum energy level of the TS. In this way, when the TSO requests upward or downward reserve, there is enough capacity available to provide it. The algorithm adjusts these margins based on the reserve that needs to be provided by the CSP. For example, if providing reserve is not favorable for the RVPP, the optimization problem relaxes these margins accordingly. It is important to note that if these margins are not considered, the RVPP may face penalization or exemption from the market due to its inability to provide the requested reserve by the TSO. For instance, at hour 10, if the energy level of the TS were at its minimum (represented by the dashed grey line), it would not be possible for the CSP to provide the requested upward reserve during this time period.

4.2. Case 2

Figure 12 shows the traded electrical energy and reserve of the RVPP in the DAM and SRM, as well as the purchased thermal energy through the HPA from the thermal service provider, while considering different uncertainties. For the optimistic decision (only a small number of hours are considered as the worst case), the RVPP purchases the lowest amount of electrical and thermal energy when it is an energy buyer in the market. Conversely, when the RVPP is a seller in the market, it sells more electrical energy. For the balanced decision, the amounts of purchased electrical and thermal energy increase, while the amount of sold electrical energy decreases compared to the optimistic decision. Specifically, during hours 5, 6, and 21, the RVPP buys more thermal energy to manage TDs uncertainties. The traded electrical energy is affected
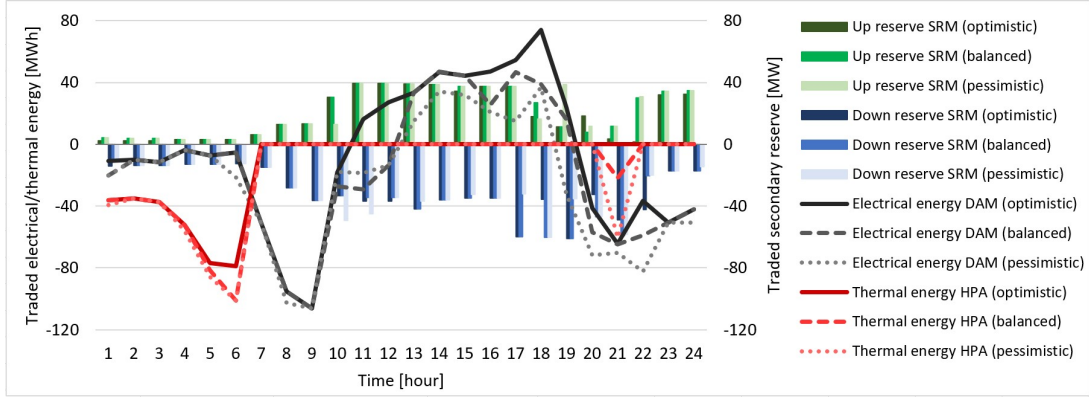
31

Figure 12: The RVPP traded electrical and thermal energy by considering different uncertainties.

in more hours compared to thermal energy, as it is influenced by multiple uncertainties, including variations in the production of WFs, solar PVs, and CSP, as well as fluctuations in EDs. Since the worst-case scenario for production or demand can occur at different hours, the hours 11, 12, 16, 18, 20, and 22 exhibit the highest deviations in traded electrical energy compared to the optimistic decision. As a significant portion of the RVPP's energy production comes from solar PVs, most of these hours correspond to periods of high volatility in solar production—morning hours (11 and 12) and evening hours (16, 18, and 20). Additionally, some hours are strongly affected by uncertainty, leading to a change in the direction of the RVPP's traded electrical energy. For example, in hours 11 and 12, the RVPP becomes an energy buyer, whereas in the optimistic decision, it was an energy seller during these hours.

For the pessimistic decision, a greater number of hours (6 or 9 out of 24, according to Table 7) are selected as the worst case for each uncertain parameter. As a result, the RVPP operator adopts a more conservative strategy. The thermal energy purchased by the RVPP through the HPA increases in hours 1, 4, 5, and 21, with a more significant increase in hour 21. In this hour, the TDs of the RVPP remain similar to those in the balanced decision. However, the RVPP prefers to purchase more thermal energy at this time to compensate for a lack of thermal energy in the CSP. This shortage of thermal energy in the CSP results from greater variations in the production and demand of other units in previous hours, which the CSP would otherwise compensate for. The RVPP is an electrical energy seller only between hours 13-18; during all other hours, it buys electrical energy from the market. The variation of traded electrical energy from the balanced to the pessimistic decision is more significant in hours 6, 13-15, 17, 19, 20, and 22 than in other hours. These hours are typically those in which RVPP units still experience moderate to high deviations in production and demand but have a subsequent effect on the objective function of the optimization problem compared to worst case hours in the balanced decisions.

Figure 12 also illustrates the changes in upward and downward reserves provided under the three decision strategies considered. In hour 10, under the pessimistic strategy, the upward reserve provided by the CSP is reduced compared to the optimistic and balanced strategies. Instead of providing upward reserve, the CSP generates more energy to meet higher levels of EDs/TDs due to uncertainty. This higher production in hour 10 enables the CSP to offer more downward reserve compared to the optimistic and balanced strategies. In hour 19, the opposite situation occurs: the RVPP provides a higher amount of upward reserve and a lower amount of downward reserve under the pessimistic strategy compared to the other two strategies. The CSP does not generate electrical energy in this hour, allowing it to allocate more capacity for upward reserve. Conversely, since the CSP is not producing energy, it cannot provide any downward reserve in this hour.
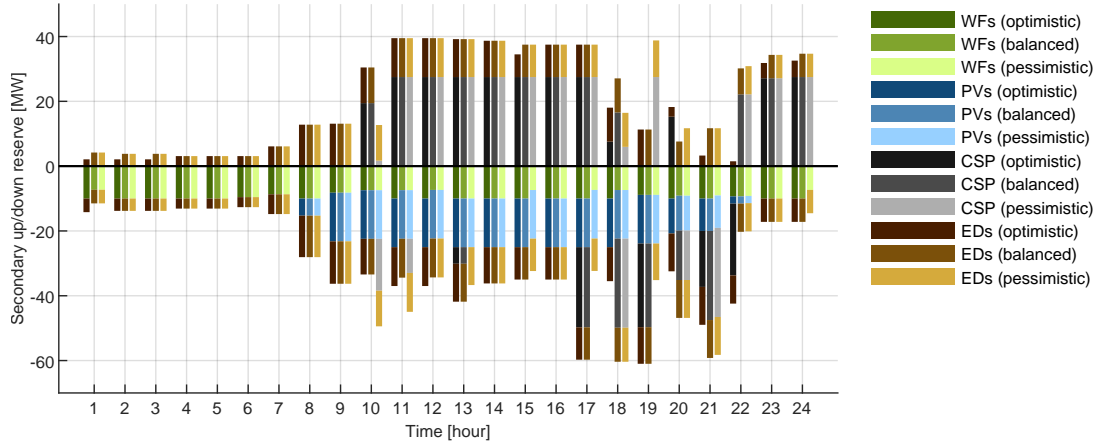
Figure 13: The RVPP units provided up and down reserve by considering different uncertainties.

To provide a more in-depth analysis of the reserve provision by the RVPP, Figure 13 presents the reserve contribution of each technology under the three strategies. The figure shows that, for all strategies, both the CSP and demands provide upward reserve. Since the production cost of solar PVs and WFs is lower than that of the CSP, they do not contribute to upward reserve provision. The CSP has a higher share than demands in providing upward reserve due to the flexibility offered by its TS. All technologies in the RVPP contribute to downward reserve provision. A significant portion of the downward reserve is supplied by solar PVs between hours 9-19 due to their high production during these hours. Between hours 17-22, the CSP provides the majority of the downward reserve, as its production level is higher in the evening. WFs contribute to downward reserve provision throughout all time periods, as they can reduce their output from the maximum production level when needed.

Table 8 compares the defined quantitative flexibility metrics for different RVPP units (as described in Section 3.2.4) under various uncertainty handling strategies. The results show that the CSP unit provides the highest contribution—measured by the reserve-to-capacity ratio—in providing upward reserve compared to other RVPP units. Furthermore, the upward reserve-to-capacity ratio is increased by adopting a more conservative strategy for both CSP and EDs, enabling them to more effectively handling uncertainty. These findings highlight the critical role of CSP in enhancing the overall flexibility of the RVPP.

A sensitivity analysis is performed to examine how varying the uncertainty budget from 0 to 24 affects the bidding strategy, reserve allocation, and overall profitability of the RVPP. The results of this analysis are presented in Figures 14 and 15. These figures illustrate that adopting a higher uncertainty budget leads the RVPP to follow a more conservative strategy—selling less electricity when acting as a seller and purchasing more when acting as a buyer in the market. This shift results in lower profitability (i.e., higher total cost) under more conservative scenarios. Additionally, the total upward and downward reserve provisions are closely linked to the volume of traded electrical and thermal energy, demonstrating the interdependence between energy trading and reserve provision. For example, under a low uncertainty budget, the upward reserve is generally lower, while the downward reserve is higher, since the RVPP tends to sell more and buy less electricity compared to scenarios with higher uncertainty budgets. Notably, for uncertainty budget values between 12 and 22, the CSP unit is turned off and does not produce electricity; as a result, it provides no reserve. In these cases, the CSP allocates most of its capacity to thermal energy provision, thereby reducing RVPP thermal energy procurement through the HPA contract.

33

Table 8: The flexibility provided by RVPP units by considering different uncertainties.

Strategy	Unit	Flexibility meteric			
		Upward reserve [MW]	Downward reserve [MW]	Upward reserve to capacity [%]	Downward reserve to capacity [%]
Optimistic	WFs	0	232.1	0	2.32
	PVs	0	193.3	0	1.29
	CSP	289.4	95.1	5.26	1.73
	EDs	171.8	209.3	0.82	1.00
Balanced	WFs	0	220.6	0	2.20
	PVs	0	193.3	0	1.29
	CSP	305.3	126.0	5.55	2.29
	EDs	204.5	209.3	0.97	1.00
Pessimistic	WFs	0	211.6	0	2.11
	PVs	0	193.3	0	1.29
	CSP	304.4	96.8	5.53	1.76
	EDs	209.3	209.3	1.00	1.00
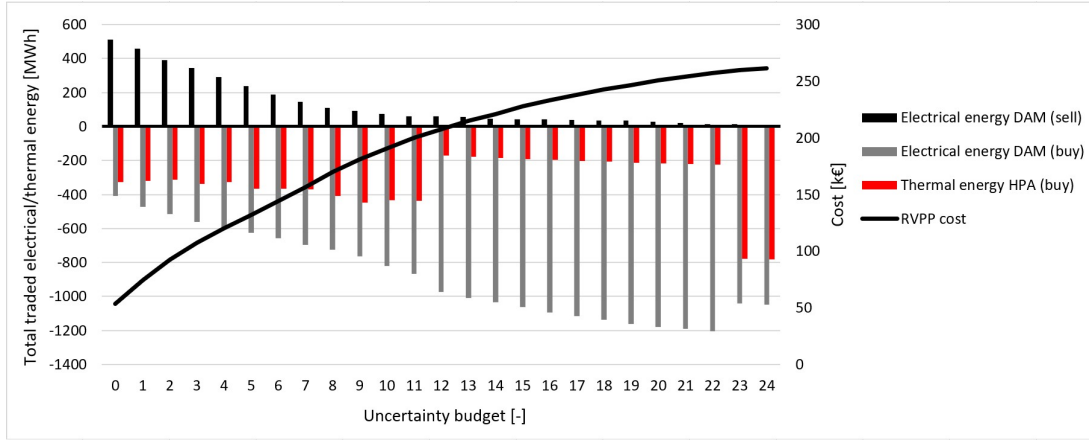
Figure 14: Sensitivity analysis for the RVPP cost as well as total traded electrical and thermal energy versus uncertainty budget.

4.3. Case 3

Table 9 presents the cost of the RVPP under different market (contract) participation strategies and different strategies for handling uncertainties. The table shows that if only DAM participation is considered, the RVPP achieves the highest cost compared to other market (contract) participation strategies. Adopting more conservative strategies against uncertainties leads to an increase in the RVPP's cost for market participation. For example, compared to the deterministic strategy, the cost increases by 67.6%, 113.5%, and 152.1% for the optimistic, balanced, and pessimistic strategies, respectively. These cost increase occur because, as more conservative strategies are implemented, the RVPP submits lower bids for selling electricity and higher bids for purchasing electricity from the DAM to ensure it can supply its demands.

When the RVPP participates in the DAM for electricity trading and also enters into a HPA contract to
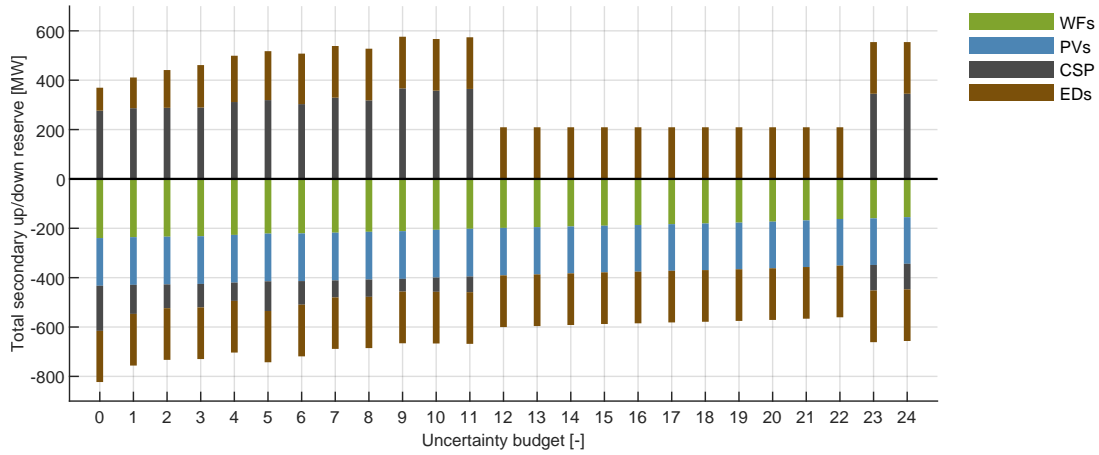
Figure 15: Sensitivity analysis for the RVPP units provided up and down reserve versus uncertainty budget.

purchase thermal energy, its cost decreases in the deterministic, optimistic, and balanced strategies by 2.0%, 1.8%, and 1.3%, respectively, compared to the DAM-only participation strategy. Since the majority of the TDs energy are supplied by the CSP of the RVPP, the cost decrease from considering the HPA is relatively marginal. However, the HPA can have a more substantial impact on costs when the HPA price is lower, when TDs require more energy, or when the CSP is unable to fully supply the energy needed for TDs. When the RVPP is allowed to participate in both the DAM and SRM, its cost decreases in the deterministic, optimistic, balanced, and pessimistic strategies by 21.7%, 10.3%, 4.4%, and 3.3%, respectively, compared to the DAM-only participation strategy. As more conservative strategies are adopted, the percentage of cost decrease inclines. Uncertainty negatively impacts both the reserve provision of the RVPP and the SRM price, thereby limiting the additional profit that can be gained from participating in the SRM. Finally, when participation in all DAM, SRM, and HPA contract is considered, the RVPP achieves its minimum cost. The cost of the RVPP decreases in the deterministic, optimistic, balanced, and pessimistic strategies by 23.9%, 12.0%, 8.3%, and 4.1%, respectively, compared to the DAM-only participation strategy.

Table 10 presents the economic analysis of the proposed RVPP without its CSP component, to more thoroughly evaluate the added value of CSP integration. The results indicate that the total cost of the RVPP with CSP—participating only in the DAM—is 58.1%, 44.4%, 38.3%, and 35.0% lower than that of the RVPP without CSP participating in all market and contract types (DAM+SRM+HPA), under the deterministic, optimistic, balanced, and pessimistic strategies, respectively. For the case where both configurations (RVPP with and without CSP) participate in all market and contract types, the cost reductions achieved with CSP integration are 68.1%, 51.1%, 43.4%, and 37.6% under the same respective strategies. These findings highlight the significant incremental value of incorporating CSP into the RVPP, particularly when it is allowed to participate in multiple energy and reserve markets.

To analyze the impact of various potential future prices of HPA (considering scenarios where thermal energy is primarily produced from renewable sources instead of fossil fuels [56]), Table 11 is presented. The table indicates that as the HPA price decreases, the cost of the RVPP also decreases. For example, when considering constant HPA prices of 70, 60, and 50 €/MWh—compared to the time-of-use HPA price in Figure 8—the cost of the RVPP decreases by 6.6%, 24.8%, and 48.9% for the deterministic strategy; 4.5%, 15.1%, and 28.8% for the optimistic strategy; 4.2%, 12.5%, and 25.2% for the balanced strategy; and 3.9%, 11.9%, and 20.7% for the pessimistic strategy. A similar trend is observed when adopting more conservative strategies, where cost reduction becomes more challenging. The results in Table 9 and Table 11 demonstrate

35

Table 9: The RVPP cost [k€] by considering different market (contract) participation strategies.

Strategy	Market (contract)			
	DAM	DAM+HPA	DAM+SRM	DAM+SRM+HPA
Deterministic	69.9	68.5	54.7	53.2
Optimistic	117.2	115.1	105.1	103.1
Balanced	149.3	147.3	142.7	136.9
Pessimistic	176.2	176.2	170.4	169.0

Table 10: The RVPP cost [k€] (without CSP) by considering different market (contract) participation strategies.

Strategy	Market (contract)	
	DAM+HPA	DAM+SRM+HPA
Deterministic	175.3	167.0
Optimistic	218.3	210.8
Balanced	248.7	242.1
Pessimistic	276.9	271.0

Table 11: The RVPP cost [k€] by considering different HPA price.

Strategy	HPA price [€/MWh]			
	Figure 8	70	60	50
Deterministic	53.2	49.7	40.0	27.2
Optimistic	103.1	98.5	87.6	73.4
Balanced	136.9	131.1	119.8	105.4
Pessimistic	169.0	160.9	148.9	134.0

that by implementing the proposed coordinated approach in the DAM, SRM, and HPA, the RVPP achieves the lowest cost, highlighting the effectiveness and practicality of the proposed approach in this paper.

Figure 16 shows the traded electrical and thermal energy of the RVPP considering different HPA prices. The results indicate that when a constant price of 70 €/MWh is assumed, the RVPP purchases thermal energy through the HPA during the morning, evening, and night hours (1–9, 11, and 18–24). Compared to the strategy with a time-of-use HPA price (Figure 8), the RVPP sells more and buys less electrical energy in the DAM, as the CSP has more thermal energy available for conversion to electrical energy rather than supplying TDs. Notably, the up secondary reserve provided by the RVPP decreases in hours 22–24, as the RVPP opts to purchase less electrical energy in the DAM. Additionally, the down secondary reserve provided by the RVPP increases in hours 9, 11, 20, and 22–24 due to higher electrical production from RVPP units. The results for lower HPA prices (60 and 50 €/MWh) show that as the HPA price decreases further, a greater portion of the RVPP's TDs is met through HPA purchases. Moreover, electrical production and down reserves provided by the RVPP increase, while the up reserve decreases. This highlights the significant impact of different thermal HPA contract prices on the electrical energy and reserve traded by the RVPP.
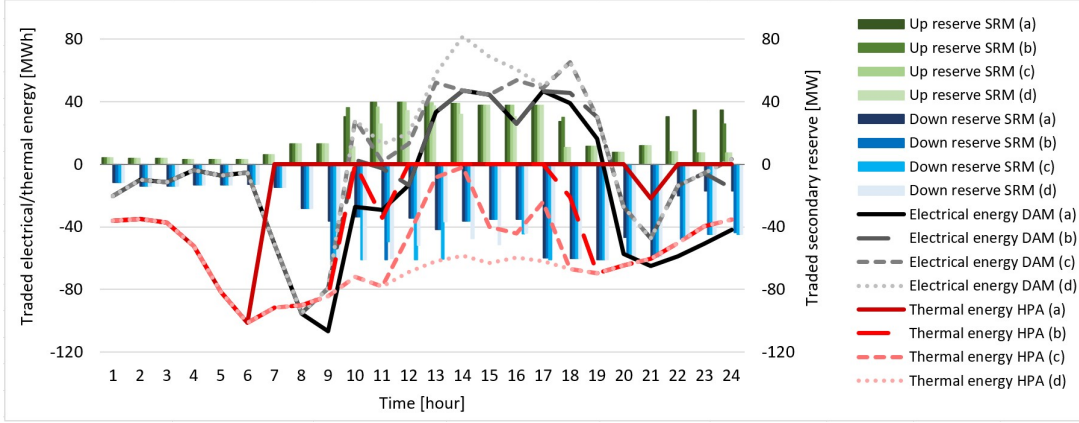
Figure 16: The RVPP traded electrical and thermal energy by considering different HPA price [€/MWh]. (a) according to Figure 8; (b) 70; (c) 60; and (d) 50 €/MWh, ∀t. Balanced strategy is considered in all cases.

4.4. Case 4

The effectiveness of the proposed approach is evaluated in comparison with the SP model from [2], using the out-of-sample method proposed in [57]. The scenario generation method used for the SP model is based on Monte Carlo simulations applied to the same historical data used to define the uncertainty bounds in the proposed approach. Moreover, separate datasets are employed for training the models and conducting the out-of-sample evaluation. Importantly, both models are assessed using an identical set of scenarios during testing, ensuring that they are exposed to the same uncertainty. This setup is designed to isolate the effects of the modeling techniques themselves, so that any observed performance differences can be attributed to methodological differences rather than inconsistencies in the testing conditions.

Table 12 summarizes the out-of-sample performance of the proposed model under various uncertainty handling strategies. Following the definitions in [57], three metrics are reported: the average sampled cost (representing market expenses excluding penalty costs), the average sampled penalty cost (due to constraint violations), and the average sampled net cost (i.e., the sum of the average cost and the penalty cost). The simulation results indicate that adopting more conservative strategies significantly reduces the penalty costs associated with the RVPP, thereby lowering the overall net cost. Specifically, compared to the deterministic strategy, the optimistic, balanced, and pessimistic strategies reduce penalty costs by 62.9%, 72.2%, and 79.0%, respectively. However, this increased robustness comes at the expense of higher average costs, which rise by 76.6%, 128.1%, and 181.9% for the same strategies. Among the strategies evaluated, the optimistic approach yields the lowest net cost, achieving a 33.8% reduction compared to the deterministic case. Additionally, the proposed model demonstrates strong computational efficiency, with solution times remaining under 2 seconds across all strategies.

Table 13 presents the out-of-sample results for the SP model proposed in [2], evaluated under varying numbers of scenarios. The SP model demonstrates fair performance in keeping the average cost of the RVPP close to that of the deterministic strategy, which yields the lowest average market participation cost. For instance, when using 5, 10, 15, 20, and 25 scenarios, the average cost increases by 29.2%, 24.0%, 38.0%, 54.4%, and 47.9%, respectively, compared to the deterministic strategy. While increasing the number of scenarios reduces the penalization cost, the extent of this reduction is less significant than that achieved by the proposed approach. Specifically, compared to the deterministic strategy, the average penalization cost is reduced by 31.2%, 35.0%, 40.6%, 48.1%, and 52.6% for 5, 10, 15, 20, and 25 scenarios, respectively. Although these reductions are notable, they remain lower than the maximum 79.0% reduction achieved

37

Table 12: The out-of-sample results for the proposed model.

Strategy	Average sampled cost [k€]	Average sampled penalization cost [k€]	Average sampled net cost [k€]	Computational time [s]
Deterministic	17.1	64.8	81.9	1.5
Optimistic	30.2	24.0	54.2	1.8
Balanced	39.0	18.0	57.0	1.0
Pessimistic	48.2	13.6	61.8	1.4

Table 13: The out-of-sample results for the model in [2].

Number of scenarios [-]	Average sampled cost [k€]	Average sampled penalization cost [k€]	Average sampled net cost [k€]	Computational time [s]
5	22.1	44.6	66.7	73.9
10	21.2	42.1	63.3	547.2
15	23.6	38.5	62.1	836.0
20	26.4	33.6	60.0	1447.2
25	25.3	30.7	56.0	6900.1

with the proposed method. Overall, while the SP model effectively maintains a low average market cost, it performs less well in capturing worst-case scenarios that lead to high penalty costs. As a result, a higher net cost is obtained with the SP approach compared to the proposed approach. Additionally, as the number of scenarios increases, the average net cost of the RVPP decreases, emphasizing the importance of selecting an appropriate number of scenarios in the SP model. The lowest net cost in the SP model is observed with 25 scenarios, amounting to 56.0 k€. However, this comes at a high computational cost, with the solution time reaching 6900 seconds.

5. Conclusion

In this paper, a new two-stage robust model is proposed for the integration of CSPs in the RVPP. The RVPP includes CSPs, WFs, solar PVs, EDs, and TDs, and trades electrical energy and reserves in the DAM and SRM, while also purchasing thermal energy to supply its local TDs. Multiple uncertainties related to electricity prices, as well as the source and load sides of RVPP production and consumption, are taken into account by incorporating temporal constraints to determine the flexible worst case in RO. The energy and reserve provision of CSP is modeled by assigning an adjustable level of energy from the TS of CSP for reserve provision. Several case studies are conducted to demonstrate the applicability and computational efficiency of the proposed approach. The simulation results show that the CSP provides electrical energy to meet demand during early morning and late evening hours when the production of solar PV plants in the RVPP is low. Additionally, the majority of the up reserve provided by the RVPP is scheduled to be supplied by the CSP due to its flexibility. Furthermore, the CSP can supply TDs during daylight hours, primarily with the help of its SF production, and supply TD during other hours when sunlight is unavailable by discharging the TS. The results show that adopting an optimistic decision by the RVPP against uncertain parameters leads to selling more electrical energy and buying less electrical and thermal energy compared to balanced and pessimistic strategies. The traded reserve in the SRM is also affected by the electrical and thermal energy traded. For example, in the pessimistic case, during some hours, since the CSP has higher electrical energy

production, its provided up and down reserves decrease and increase, respectively. The results also show that by adopting the proposed coordinated strategy (DAM + SRM + HPA), the cost of the RVPP decreases by 4.1%–23.9% compared to the DAM-only participation strategy. Additionally, the effect of different HPA prices on traded thermal energy and the profitability of the RVPP is analyzed. The results indicate that for lower HPA prices, the purchased thermal energy through HPA increases. The cost of the RVPP for an HPA price of 50 €/MWh decreases by 20.7%–48.9% for different RVPP strategies against uncertainties compared to the assumed time-of-use price for HPA.

Future work would focus on modeling and analyzing the potential spatiotemporal correlations among uncertain parameters, and how they can influence RVPP performance.

Appendix A. CSP Turn On/Off Constraints

The minimum up and down time constraints for turbine of CSP are formulated in (A.1) and are adopted from [58]. Constraints (A.1a) and (A.1b) define the commitment status of turbine. The parameters N_θ^{ON} and N_θ^{OFF} are the number of initial periods during which turbine must be online/offline, respectively. Equation (A.1c) defines the initial status of turbine as defined by N_θ^{ON}. Constraint (A.1d) restricts the minimum up time during all combination of the subsequent periods UT_θ. Constraint (A.1e) defines the minimum up time for the final periods $UT_\theta - 1$. Constraints (A.1f)-(A.1h) are the minimum down time version of (A.1c)-(A.1e). The nature of binary variables is shown in (A.1i).

$$u_{\theta,t} - u_{\theta,t-1} = v_{\theta,t}^{SU} - v_{\theta,t}^{SD} \ ; \qquad\qquad \forall \theta, t \in \Theta, \mathcal{T} \qquad (A.1a)$$

$$v_{\theta,t}^{SU} + v_{\theta,t}^{SD} \leq 1 \ ; \qquad\qquad \forall \theta, t \in \Theta, \mathcal{T} \qquad (A.1b)$$

$$\sum_{t=1}^{N_\theta^{ON}} [1 - u_{\theta,t}] = 0 \ ; \qquad\qquad \forall \theta \in \Theta \qquad (A.1c)$$

$$UT_\theta (u_{\theta,t} - u_{\theta,t-1}) \leq \sum_{t'=t}^{t+UT_\theta-1} u_{\theta,t'} \ ; \qquad\qquad \forall \theta \in \Theta, t = N_\theta^{ON} + 1, ..., |\mathcal{T}| - UT_\theta + 1 \qquad (A.1d)$$

$$0 \leq \sum_{t'=t}^{|\mathcal{T}|} [u_{\theta,t'} - (u_{\theta,t} - u_{\theta,t-1})] \ ; \qquad\qquad \forall \theta \in \Theta, t = |\mathcal{T}| - UT_\theta + 2, ..., |\mathcal{T}| \qquad (A.1e)$$

$$\sum_{t=1}^{N_\theta^{OFF}} u_{\theta,t} = 0 \ ; \qquad\qquad \forall \theta \in \Theta \qquad (A.1f)$$

$$DT_\theta (u_{\theta,t-1} - u_{\theta,t}) \leq \sum_{t'=t}^{t+DT_\theta-1} [1 - u_{\theta,t'}] \ ; \qquad\qquad \forall \theta \in \Theta, t = N_\theta^{OFF} + 1, ..., |\mathcal{T}| - DT_\theta + 1 \qquad (A.1g)$$

$$0 \leq \sum_{t'=t}^{|\mathcal{T}|} [1 - u_{\theta,t'} - (u_{\theta,t-1} - u_{\theta,t})] \ ; \qquad\qquad \forall \theta \in \Theta, t = |\mathcal{T}| - DT_\theta + 2, ..., |\mathcal{T}| \qquad (A.1h)$$

$$u_{\theta,t}, v_{\theta,t}^{SU}, v_{\theta,t}^{SD} \in \{0, 1\} \ ; \qquad\qquad \forall \theta, t \in \Theta, \mathcal{T} \qquad (A.1i)$$

Acknowledgments

References

[1] R. Dominguez, L. Baringo, A. Conejo, Optimal offering strategy for a concentrating solar power plant, Applied Energy 98 (2012) 316–325.

[2] Y. Zhao, S. Liu, Z. Lin, F. Wen, Y. Ding, Coordinated scheduling strategy for an integrated system with concentrating solar power plants and solar prosumers considering thermal interactions and demand flexibilities, Applied Energy 304 (2021) 117646.

[3] U.S. Department of Energy, Concentrating solar power (2023).
URL https://www.energy.gov/eere/solar/concentrating-solar-power

[4] I. L. García, J. L. Álvarez, D. Blanco, Performance model for parabolic trough solar thermal power plants with thermal storage: Comparison to operating plant data, Solar Energy 85 (10) (2011) 2443–2460.

[5] D. Miron, A. Navon, Y. Levron, J. Belikov, C. Rotschild, The cost-competitiveness of concentrated solar power with thermal energy storage in power systems with high solar penetration levels, Journal of Energy Storage 72 (2023) 108464.

[6] I. R. E. A. (IRENA), Renewable energy benefits: Leveraging local capacity for concentrated solar power, Tech. rep., International Renewable Energy Agency (IRENA), Abu Dhabi (2025).
URL https://www.irena.org/-/media/Files/IRENA/Agency/Publication/2025/Jan/IRENA_Renewable_energy_benefits_leveraging_capacity_CSP_2025.pdf

[7] M. I. Khan, F. Asfand, S. G. Al-Ghamdi, Progress in research and technological advancements of thermal energy storage systems for concentrated solar power, Journal of Energy Storage 55 (2022) 105860.

[8] L. Yao, Y. Wang, X. Xiao, Concentrated solar power plant modeling for power system studies, IEEE Transactions on Power Systems (2023).

[9] Á. Ortega, O. Oladimeji, H. Nemati, L. Sigrist, P. Sánchez-Martín, L. Rouco, E. Lobato, M. Biencinto, I. López, Modeling of VPPs for their optimal operation and configuration, Tech. rep., POSYTYF Consortium, deliverable 5.1. (2021).

[10] A. J. Conejo, M. Carrión, J. M. Morales, et al., Decision making under uncertainty in electricity markets, Vol. 1, Springer, 2010.

[11] N. Naval, J. M. Yusta, Virtual power plant models and electricity markets-A review, Renewable and Sustainable Energy Reviews 149 (2021) 111393.

[12] C. Fernandes, P. Frías, J. Reneses, Participation of intermittent renewable generators in balancing mechanisms: A closer look into the spanish market design, Renewable Energy 89 (2016) 305–316.

[13] S. Sun, S. M. Kazemi-Razi, L. G. Kaigutha, M. Marzband, H. Nafisi, A. S. Al-Sumaiti, Day-ahead offering strategy in the market for concentrating solar power considering thermoelectric decoupling by a compressed air energy storage, Applied Energy 305 (2022) 117804.

[14] X. Kong, J. Xiao, D. Liu, J. Wu, C. Wang, Y. Shen, Robust stochastic optimal dispatching method of multi-energy virtual power plant considering multiple uncertainties, Applied Energy 279 (2020) 115707.

[15] F. Ghasemi Olanlari, T. Amraee, M. Moradi-Sepahvand, A. Ahmadian, Coordinated multi-objective scheduling of a multi-energy virtual power plant considering storages and demand response, IET Generation, Transmission & Distribution 16 (17) (2022) 3539–3562.

[16] M. Foroughi, A. Pasban, M. Moeini-Aghtaie, A. Fayaz-Heidari, A bi-level model for optimal bidding of a multi-carrier technical virtual power plant in energy markets, International Journal of Electrical Power & Energy Systems 125 (2021) 106397.

[17] L. Wang, W. Gu, Z. Wu, H. Qiu, G. Pan, Non-cooperative game-based multilateral contract transactions in power-heating integrated systems, Applied Energy 268 (2020) 114930.

[18] S. Hasni, W. J. Platzer, Case study on decarbonization strategies for LNG export terminals using heat and power from CSP/PV hybrid plants, Solar Energy Advances 3 (2023) 100041.

[19] K. J. Kircher, K. M. Zhang, Heat purchase agreements could lower barriers to heat pump adoption, Applied Energy 286 (2021) 116489.

[20] L. A. Roald, D. Pozo, A. Papavasiliou, D. K. Molzahn, J. Kazempour, A. Conejo, Power systems optimization under uncertainty: A review of methods and applications, Electric Power Systems Research 214 (2023) 108725.

[21] V. Singh, T. Moger, D. Jena, Uncertainty handling techniques in power systems: A critical review, Electric Power Systems Research 203 (2022) 107633.

[22] J. F. Venegas-Zarama, J. I. Muñoz-Hernandez, L. Baringo, P. Diaz-Cachinero, I. De Domingo-Mondejar, A review of the evolution and main roles of virtual power plants as key stakeholders in power systems, IEEE Access 10 (2022) 47937–47964.

[23] H. Xiong, F. Luo, M. Yan, L. Yan, C. Guo, G. Ranzi, Distributionally robust and transactive energy management scheme for integrated wind-concentrated solar virtual power plants, Applied Energy 368 (2024) 123148.

[24] S. Yu, F. Fang, Y. Liu, J. Liu, Uncertainties of virtual power plant: Problems and countermeasures, Applied energy 239 (2019) 454–470.

[25] H. Nemati, P. Sánchez-Martín, Á. Ortega, L. Sigrist, E. Lobato, L. Rouco, Flexible robust optimal bidding of renewable virtual power plants in sequential markets under asymmetric uncertainties, Sustainable Energy, Grids and Networks (2025) 101801.

[26] M. Rahimi, F. J. Ardakani, A. J. Ardakani, Optimal stochastic scheduling of electrical and thermal renewable and non-renewable resources in virtual power plant, International Journal of Electrical Power & Energy Systems 127 (2021) 106658.

[27] D. Xiao, Z. Lin, H. Chen, W. Hua, J. Yan, Windfall profit-aware stochastic scheduling strategy for industrial virtual power plant with integrated risk-seeking/averse preferences, Applied Energy 357 (2024) 122460.

[28] N. T. Kalantari, A. Abdolahi, S. H. Mousavi, S. C. Khavar, F. S. Gazijahani, Strategic decision making of energy storage owned virtual power plant in day-ahead and intra-day markets, Journal of Energy Storage 73 (2023) 108839.

[29] Y. Li, Y. Deng, Y. Wang, L. Jiang, M. Shahidehpour, Robust bidding strategy for multi-energy virtual power plant in peak-regulation ancillary service market considering uncertainties, International Journal of Electrical Power & Energy Systems 151 (2023) 109101.

[30] M. Gough, S. F. Santos, M. S. Javadi, J. M. Home-Ortiz, R. Castro, J. P. Catalão, Bi-level stochastic energy trading model for technical virtual power plants considering various renewable energy sources, energy storage systems and electric vehicles, Journal of Energy Storage 68 (2023) 107742.

[31] H. Nemati, P. Sánchez-Martín, A. Baringo, Á. Ortega, Single-level flexible robust optimal bidding of renewable-only virtual power plant in energy and secondary reserve markets, Energy 328 (2025) 136421.

[32] H. Nemati, P. Sánchez-Martín, L. Sigrist, L. Rouco, Á. Ortega, Flexible robust optimization for renewable-only VPP bidding on electricity markets with economic risk analysis, International Journal of Electrical Power & Energy Systems 167 (2025) 110594.

[33] Q. Yan, M. Zhang, H. Lin, W. Li, Two-stage adjustable robust optimal dispatching model for multi-energy virtual power plant considering multiple uncertainties and carbon trading, Journal of cleaner production 336 (2022) 130400.

[34] Y. Zhao, S. Liu, Z. Lin, F. Wen, L. Yang, Q. Wang, A mixed CVaR-based stochastic information gap approach for building optimal offering strategies of a CSP plant in electricity markets, IEEE Access 8 (2020) 85772–85783.

[35] G. He, Q. Chen, C. Kang, Q. Xia, Optimal offering strategy for concentrating solar power plants in joint energy, reserve and regulation markets, IEEE Transactions on sustainable Energy 7 (3) (2016) 1245–1254.

[36] T. Xu, N. Zhang, Coordinated operation of concentrated solar power and wind resources for the provision of energy and reserve services, IEEE Transactions on Power Systems 32 (2) (2016) 1260–1271.

[37] H. Xiong, M. Yan, C. Guo, Y. Ding, Y. Zhou, DP based multi-stage ARO for coordinated scheduling of CSP and wind energy with tractable storage scheme: Tight formulation and solution technique, Applied Energy 333 (2023) 120578.

[38] H. M. I. Pousinho, H. Silva, V. Mendes, M. Collares-Pereira, C. P. Cabrita, Self-scheduling for energy and spinning reserve of wind/CSP plants by a MILP approach, Energy 78 (2014) 524–534.

[39] Y. Fang, S. Zhao, Look-ahead bidding strategy for concentrating solar power plants with wind farms, Energy 203 (2020) 117895.

[40] H. Khaloie, F. Vallée, C. S. Lai, J.-F. Toubeau, N. D. Hatziargyriou, Day-ahead and intraday dispatch of an integrated biomass-concentrated solar system: A multi-objective risk-controlling approach, IEEE Transactions on Power Systems 37 (1) (2021) 701–714.

[41] O. Oladimeji, Á. Ortega, L. Sigrist, L. Rouco, P. Sánchez-Martín, E. Lobato, Optimal participation of heterogeneous, RES-based virtual power plants in energy markets, Energies 15 (9) (2022) 3207.

[42] Q. Fang, N. Liang, Z. Liu, M. Miao, Optimization scheduling of virtual power plant with concentrated solar power plant considering carbon trading and demand response, in: 2023 IEEE International Conference on Power Science and Technology (ICPST), IEEE, 2023, pp. 717–722.

[43] D. Bertsimas, M. Sim, The price of robustness, Operations Research 52 (1) (2004) 35–53.

[44] Z. Zhang, M. Zhou, Z. Wu, S. Liu, Z. Guo, G. Li, A frequency security constrained scheduling approach considering wind farm providing frequency support and reserve, IEEE Transactions on Sustainable Energy 13 (2) (2022) 1086–1100.

[45] S. Yin, J. Wang, Z. Li, X. Fang, State-of-the-art short-term electricity market operation with solar generation: A review, Renewable and Sustainable Energy Reviews 138 (2021) 110647.

[46] O. Oladimeji, A. Ortega, L. Sigrist, P. Sánchez-Martín, E. Lobato, L. Rouco, Modeling demand flexibility of RES-based virtual power plants, in: 2022 IEEE Power & Energy Society General Meeting (PESGM), IEEE, 2022, pp. 1–5.

[47] X. Chen, M. Sim, P. Sun, A robust optimization perspective on stochastic programming, Operations research 55 (6) (2007) 1058–1071.

[48] C. A. Floudas, Nonlinear and mixed-integer optimization: fundamentals and applications, Oxford University Press, 1995.

[49] J. Wang, Z. Hu, S. Xie, Expansion planning model of multi-energy system with the integration of active distribution network, Applied Energy 253 (2019) 113517.

[50] A. Srinivasan, R. Wu, P. Heer, G. Sansavini, Impact of forecast uncertainty and electricity markets on the flexibility provision and economic performance of highly-decarbonized multi-energy systems, Applied Energy 338 (2023) 120825.

[51] Y. Wen, D. AlHakeem, P. Mandal, S. Chakraborty, Y.-K. Wu, T. Senjyu, S. Paudyal, T.-L. Tseng, Performance evaluation of probabilistic methods based on bootstrap and quantile regression to quantify PV power point forecast uncertainty, IEEE transactions on neural networks and learning systems 31 (4) (2019) 1134–1144.

[52] Ciemat Spain, PV-STU production forecast.
URL https://www.ciemat.es/

[53] Iberdrola Spain, Wind production forecast.
URL https://www.iberdrola.es/.

[54] SCCER JASM Data Platform, Demand Hourly Profile (2019).
URL https://data.sccer-jasm.ch/demand-hourly-profile/2019-02-27/

[55] Red Eléctrica de España (REE), Electricity Market Data.
URL https://www.esios.ree.es/

[56] Statista, Levelized cost of heat in spain by technology (2024).
URL https://www.statista.com/statistics/1534706/levelized-cost-of-heat-spain\
-by-technology/

[57] A. Baringo, L. Baringo, J. M. Arroyo, Day-ahead self-scheduling of a virtual power plant in energy and reserve electricity markets under uncertainty, IEEE Transactions on Power Systems 34 (3) (2018) 1881–1894.

[58] M. Carrión, J. M. Arroyo, A computationally efficient mixed-integer linear formulation for the thermal unit commitment problem, IEEE Transactions on power systems 21 (3) (2006) 1371–1378.